NASA TECHNICAL NOTE

NASA TN D-3822

NASA TN D-3822

EXPERIMENTAL INVESTIGATION OF ACOUSTIC LINERS TO SUPPRESS SCREECH IN HYDROGEN-OXYGEN ROCKETS

by John P. Wanhainen, Harry E. Bloomer, David W. Vincent, and Jerome K. Curley

Lewis Research Center
Cleveland, Ohio

NATIONAL AERONAUTICS AND SPACE ADMINISTRATION • WASHINGTON, D. C. • FEBRUARY 1967

NASA TN D-3822

EXPERIMENTAL INVESTIGATION OF ACOUSTIC LINERS TO SUPPRESS SCREECH IN HYDROGEN-OXYGEN ROCKETS

By John P. Wanhainen, Harry E. Bloomer,
David W. Vincent, and Jerome K. Curley

Lewis Research Center
Cleveland, Ohio

NATIONAL AERONAUTICS AND SPACE ADMINISTRATION

For sale by the Clearinghouse for Federal Scientific and Technical Information
Springfield, Virginia 22151 – Price $2.00

EXPERIMENTAL INVESTIGATION OF ACOUSTIC LINERS TO SUPPRESS SCREECH IN HYDROGEN-OXYGEN ROCKETS

by John P. Wanhainen, Harry E. Bloomer, David W. Vincent, and Jerome K. Curley

Lewis Research Center

SUMMARY

An investigation of suppression of high frequency combustion instability using Helmholtz type acoustic damping devices was conducted at the Lewis Research Center in a hydrogen-oxygen rocket of nominally 20 000-pound thrust size. Acoustic liner design variables investigated include the number and the diameter of the apertures, the thickness of the liner, the length of the liner, and the gap height behind the liner. The tests were conducted at a chamber pressure (nominal) of 300 pounds per square inch absolute and a range of oxidant-fuel ratios from 4 to 6. Hydrogen injection temperature was used to rate the stability of the various liners. The liner with the lowest self-triggering temperature was considered to be the most stable design.

High frequency combustion instability in hydrogen-oxygen engines of the size investigated can be suppressed using a properly designed array of Helmholtz resonators. The hydrogen temperature at which screech occurred could be reduced from 112° to less than 60° R (minimum available) by incorporating an acoustic liner with a calculated absorption coefficient of 0.25 or greater. Analytical predictions based on acoustic theory were in limited agreement with experimental results providing a flow past the apertures of 0.2 free stream velocity was included in the calculation of absorption coefficient. Liner cavity gas temperature varied from 600° to 1000° R during stable combustion depending on the number of apertures and increased to 2000° R during screeching combustion. A 17 percent partial length liner positioned at the injector end of the thrust chamber had the same stability characteristics as the full length liner.

INTRODUCTION

Screech may be regarded as a state which exists when energy excitation exceeds energy absorption. Accordingly, two approaches to eliminate screech are suggested, (1) decrease acoustic energy generation or (2) increase acoustic absorption. The use of

acoustic liners represents one approach in increasing energy absorption and has the merit of probably being effective irrespective of the propellant combination. Because of the probable universality of such a solution, considerable effort has been expended at the Lewis Research Center on acoustic liners (ref. 1).

The use of acoustic liners of the Helmholtz type to suppress high frequency instability in combustion chambers has been successfully demonstrated in ramjet and afterburning turbojet applications (refs. 2 to 4) and in rocket engine thrust chambers (refs. 5 and 6). However, the problem still exists of adapting Helmholtz resonator theory to the conditions in a screeching rocket engine. The purpose of this investigation was to determine the effects of several design variables on the absorption characteristics of multiple resonator liners and incorporate these results in the development of a design procedure for liners.

The investigation reported herein was conducted in the Rocket Engine Test Facility using a liquid hydrogen-oxygen rocket which was 10.78 inches in diameter. The engine was operated at a chamber pressure of 300 pounds per square inch and produced a sea level thrust of about 20 000 pounds. The effects of changes in liner design parameters were evaluated by ramping the hydrogen injection temperature down into screech and determining the improvement in hydrogen temperature stable operating limits. The configuration with the lowest self-triggering temperature was considered the most stable design. The rating criterion and the hydrogen temperature ramping technique were obtained from reference 7. The design variables investigated included the number and the diameter of the apertures, the thickness of the liner, the length of the liner, and the gap height behind the liner. The basic injector was selected to have poor stability characteristics (a high screech transition hydrogen temperature) to provide a severe test for the liners. The design of the Helmholtz resonator arrays used in this investigation was based on the work of Blackman (ref. 8) and Ingaard (ref. 9) as modified by Pratt & Whitney Aircraft Corporation (unpublished data from G. E. Canuel).

SYMBOLS

A_f amplitude parameter, sec/ft

a aperture spacing, in.

c velocity of sound for resonator, ft/sec

d aperture or orifice diameter, in.

f screech or design frequency, cps

f_o liner resonator frequency, cps

g conversion factor, 32.174 $(lb_m)(ft)/(lb_f)(sec^2)$

L	liner backing distance, in.
l_{eff}	effective mass vibrating in neck of resonator, in.
O/F	oxidant-fuel ratio
P_i	pressure amplitude of incident wave (zero to peak), lb_f/sq ft
Q	bandwidth factor, dimensionless
R	gas constant, 1545 $(lb_m/sq\ ft)(cu\ ft)/(lb_{mole})(^oR)$
r_d	acoustic friction resistance, $lb_m/(sq\ ft)(sec)$
r_r	acoustic radiation resistance, $lb_m/(sq\ ft)(sec)$
T	gas temperature behind liner, ^oR
t	liner thickness, in.
U	flow velocity past orifice, ft/sec
V	flow velocity through orifice, ft/sec
X_o	particle displacement, in.
x	specific acoustic reactance ratio, dimensionless
α	absorption coefficient, dimensionless
Δ_{nl}	nonlinear resistance term, in.
δ	effective length correction factor, ft
ϵ	nonlinear resistance parameter, dimensionless
θ	specific acoustic resistance ratio, dimensionless
μ	viscosity of fluid in volume of resonator, $lb_m/(sec)(ft)$
ρ	density of fluid in volume of resonator, lb_m/cu ft
σ	fraction of open area of resonator array, $\pi d^2/4a^2$
ω	design or screech frequency, rad/sec

Subscripts:

H_2	hydrogen
O_2	oxygen
o	resonant

APPARATUS

Facility

The Rocket Engine Test Facility of the Lewis Research Center is a 50 000-pound sea level thrust stand equipped with an exhaust gas scrubber and muffler. The engine was mounted on the thrust stand (fig. 1) to fire vertically into the scrubber where the exhaust products were sprayed with water at rates of 50 000 gallons per minute for the purpose of cooling and sound suppression. The cooled exhaust gases were discharged into the atmosphere from the top of a 70-foot-high exhaust stack.

The facility utilized a pressurized propellant system to deliver propellants to the engine from the storage area. The propellant storage tanks consisted of a 75-cubic-foot liquid hydrogen Dewar, a 120 000-standard-cubic-foot gaseous hydrogen high pressure bottle farm and a 55-cubic-foot liquid oxygen tank submerged in a liquid nitrogen bath.

Engine

The engine used in the investigation was a nominally 20 000-pound sea level thrust size. It consisted of a concentric tube injector, a 10.78-inch heat-sink thrust chamber liner with resonator cavities, a thrust chamber jacket, and a convergent-divergent heat-sink exhaust nozzle with a contraction ratio of 1.89 and an expansion area ratio of 1.3. The individual engine components were flanged to allow disassembly for acoustic liner changes. The length of the combustor from the injector face to the throat was 18 inches. The hot gas surfaces of the mild steel heat-sink exhaust nozzle were coated with zirconium oxide to reduce the heat transfer into the metal.

Liners

The thrust chamber acoustic liners were initially fabricated from 3/4-inch-thick oxygen-free copper. The design was dictated by a heat-sink requirement for a 3-second-duration test assuming a liner cavity gas temperature of 5000° R. Initial tests indicated a very much lower heat load than assumed for the original design; accordingly, less expensive mild steel was used to fabricate the remaining configurations. The hot gas side of each mild steel liner was coated with flame-sprayed zirconium oxide. Photographs of the copper and steel liners are presented in figure 2. The liner configurations evaluated are identified in table I.

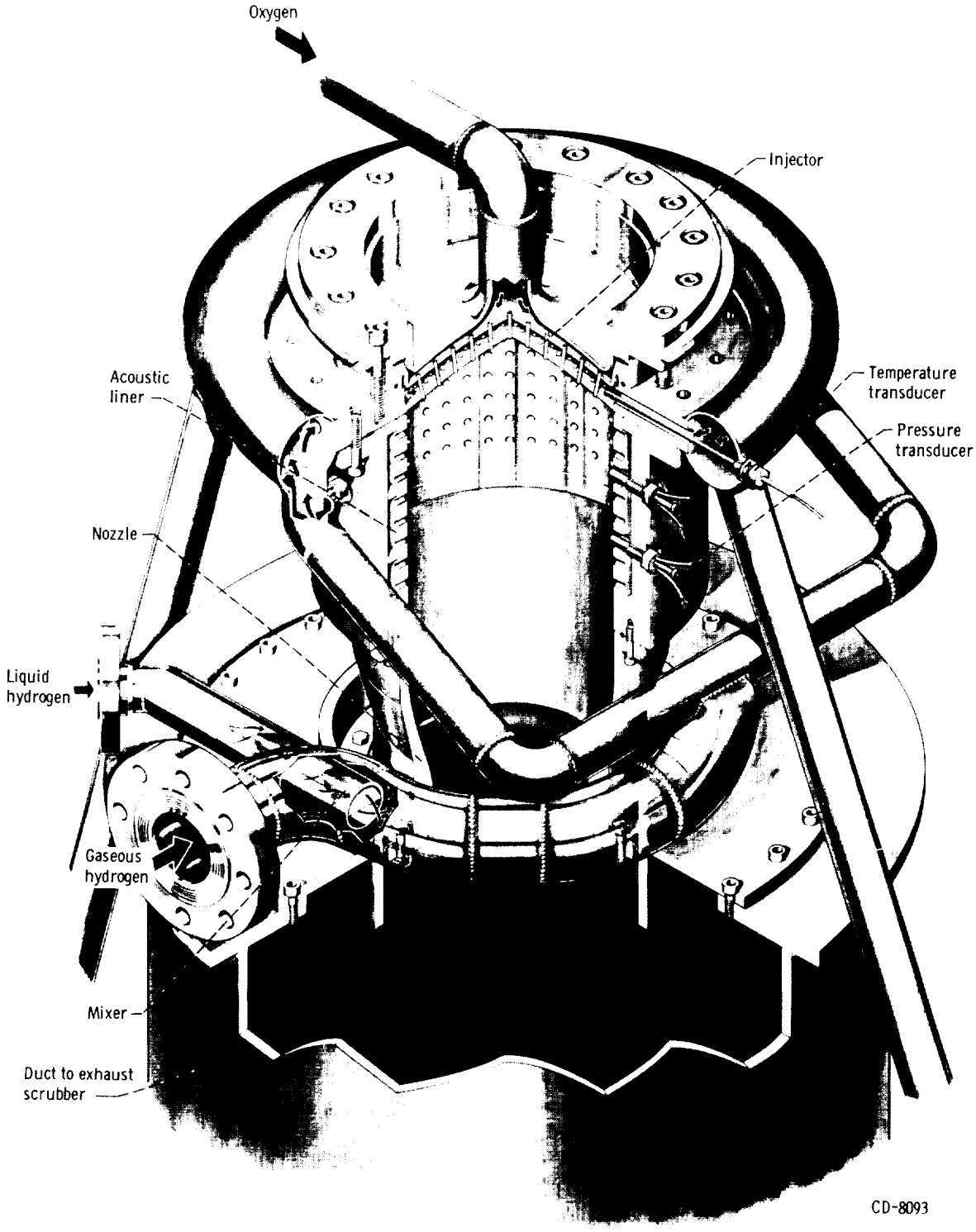

Figure 1. - Engine.

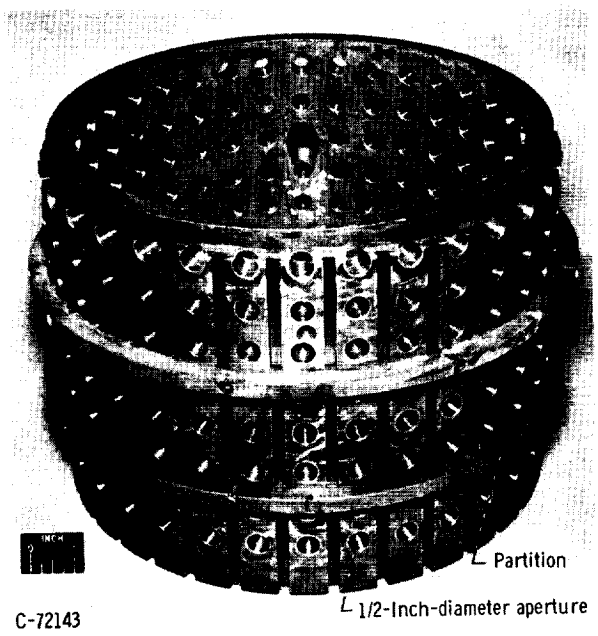

(a) 3/4-Inch-thick copper.

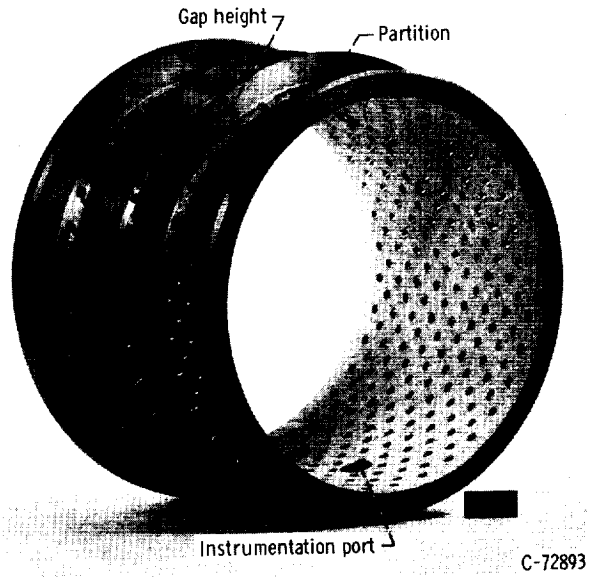

(b) 3/16-Inch-thick steel.

Figure 2. - Liner.

TABLE I. - TEST CONFIGURATIONS

Wall thickness, t, in.	Backing distance, L, in.	Aperture diameter, d, in.	Open area ratio, [a] σ	Liner length from injector, in.	Material
3/4	0.41	1/4	0.05	9	Copper
3/4	.41	1/2	.20	↓	Copper
3/8	.785	1/8	.10	↓	Copper
3/16	.9745	1/4	.05	↓	Steel
3/16	↓	↓	.10	↓	↓
3/16	↓	↓	.15	↓	↓
3/16	↓	↓	.20	↓	↓
3/16	↓	↓	.10	1.5	↓
3/16	↓	↓	.10	3.0	↓
3/16	↓	↓	.10	4.5	↓

[a] Fraction of open area of resonator array.

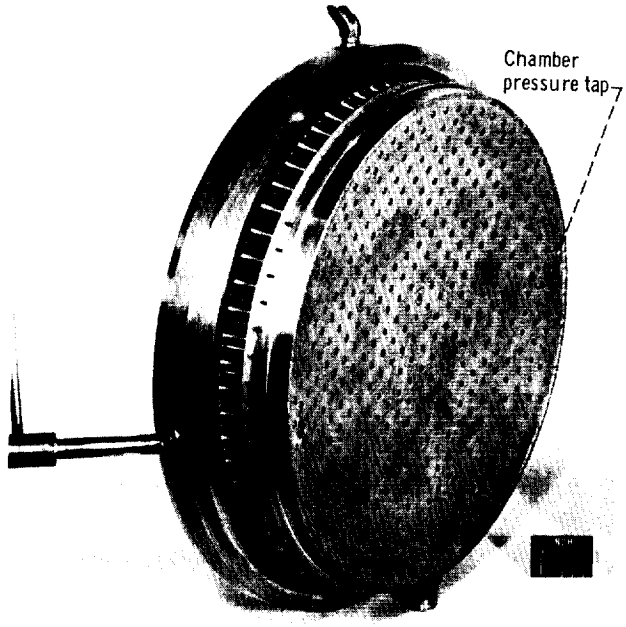

(a) Faceplate view.

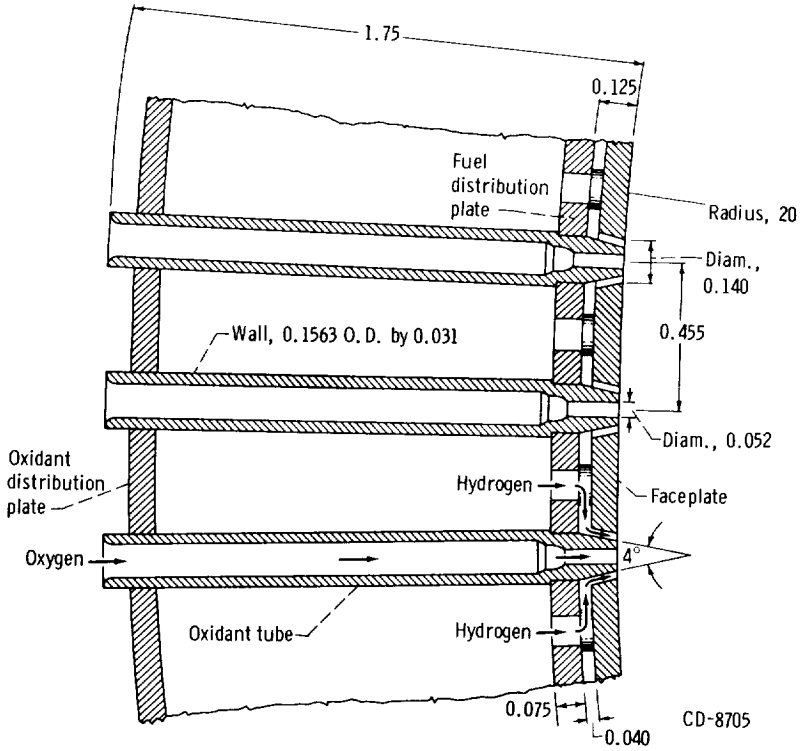

(b) Cross-sectional view. (All dimensions in inches unless specified otherwise.)

Figure 3. - Faceplate and cross-sectional views of 487-element injector.

Injector

Faceplate and cross-sectional views of the 487-element concentric tube injector (thrust per element of about 40 lb) are presented in figure 3. The faceplate was fabricated from 0.085-inch-thick nickel material formed in a concave shape with a radius of curvature of 20 inches. The injector also incorporated a hydrogen distribution plate to provide a high coolant velocity behind the faceplate for efficient cooling. The hydrogen to oxygen injection area ratio was 4.67. Element dimensions and other injector details are included in figure 3(b). All thrust chamber acoustic liners were evaluated with this injector configuration.

Hydrogen Temperature Controller

The temperature of the hydrogen entering the injector was varied by mixing various amounts of liquid and (ambient) gaseous hydrogen. A schematic of the mixing device used in the investigation is shown in figure 4. Mixing was accomplished by swirling the liquid

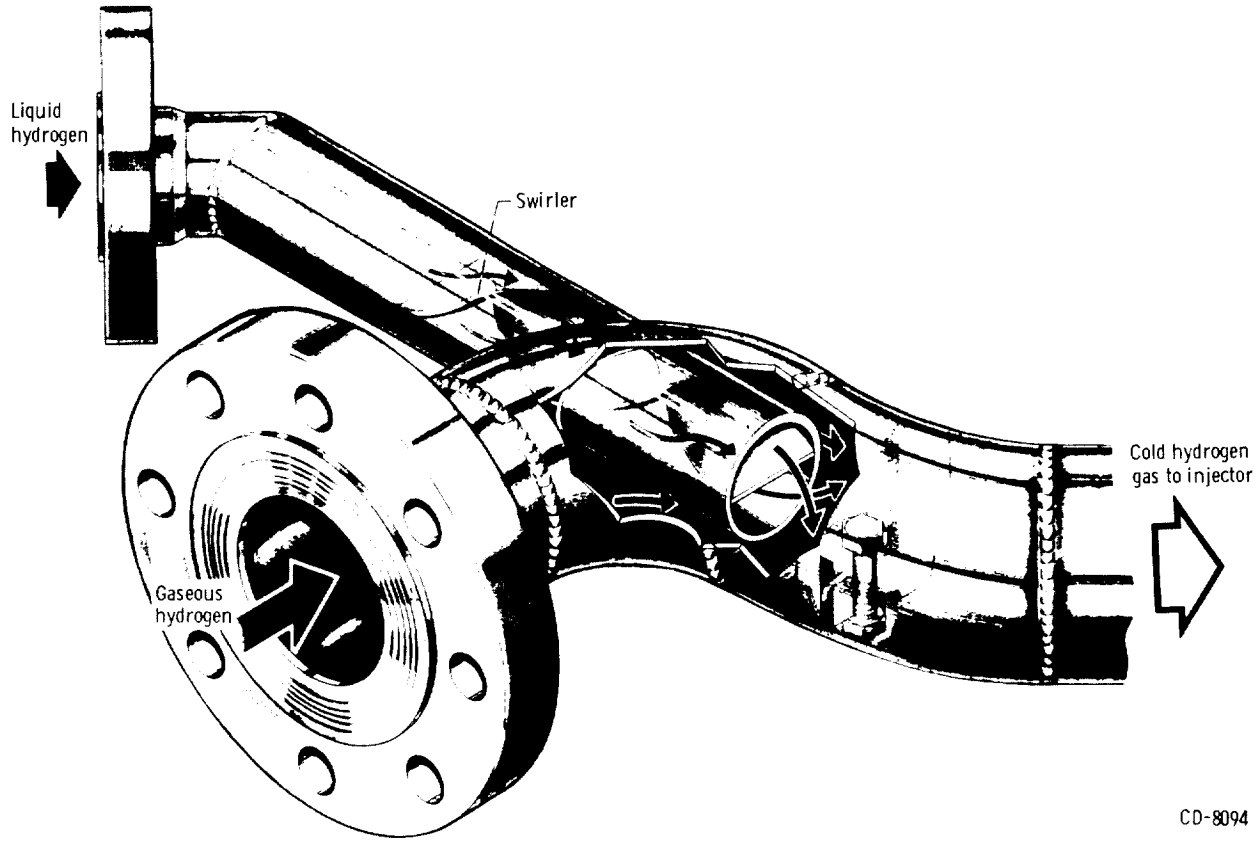

Figure 4. - Schematic of mixing station.

into the gaseous hydrogen stream. This system could reduce the hydrogen injector inlet temperature in a typical run by as much as 25° R per second. The position of the valves used to control the flow rate of gas and liquid was controlled by an electrohydraulic servosystem. Temperature ramps were accomplished by varying the signal voltage to the servovalve control amplifier by means of a potentiometer.

Instrumentation

The instrumentation used in the investigation and locations for the various transducers are shown in a diagram of the engine and associated plumbing in figure 5. The signals from the transducers, except the high frequency response types, were transmitted to the Center's automatic digital data recording system. Piezoelectric-type, water-cooled, flush-mounted pressure transducers were used at three locations on the thrust chamber to determine the character and phase relation of the pressure field and allow identification of the screech mode. The response characteristics of the transducers were flat to within 10 percent to a frequency of 6000 cps and had a nominal resonant frequency of about 20 000 cps in the water-cooled mount. The signals from high frequency response transducers were recorded in analog form on magnetic tape, and, in addition, were displayed on direct reading instruments for visual monitoring during the tests.

Oxygen propellant weight flow was determined with a vane-type flowmeter which was calibrated with water using a static weighing system. The correction from water calibration to cryogenic calibration necessitated by the dimensional change of the instrument with temperature was obtained from the flowmeter manufacturer. Liquid hydrogen weight flow was measured using a venturi, and the gaseous hydrogen weight flow was measured using an orifice plate. The strain-gage-type pressure transducers were calibrated against a commercial standard. Liquid flow temperatures were measured by platinum resistance-type sensors. The pressure and temperature systems were calibrated immediately prior to data acquisition by an electrical two-step calibration system, which used resistances in an electrical circuit to simulate a given pressure.

Procedure

As mentioned in the INTRODUCTION, the stability rating of each configuration was expressed in terms of the hydrogen temperature at which screech was encountered. The technique employed was to select an initial hydrogen temperature by presetting the valves of the mixer and, about 1/2 second after ignition, ramping the gas valve toward a closed position and the liquid valve toward an open position to reduce the temperature of the in-

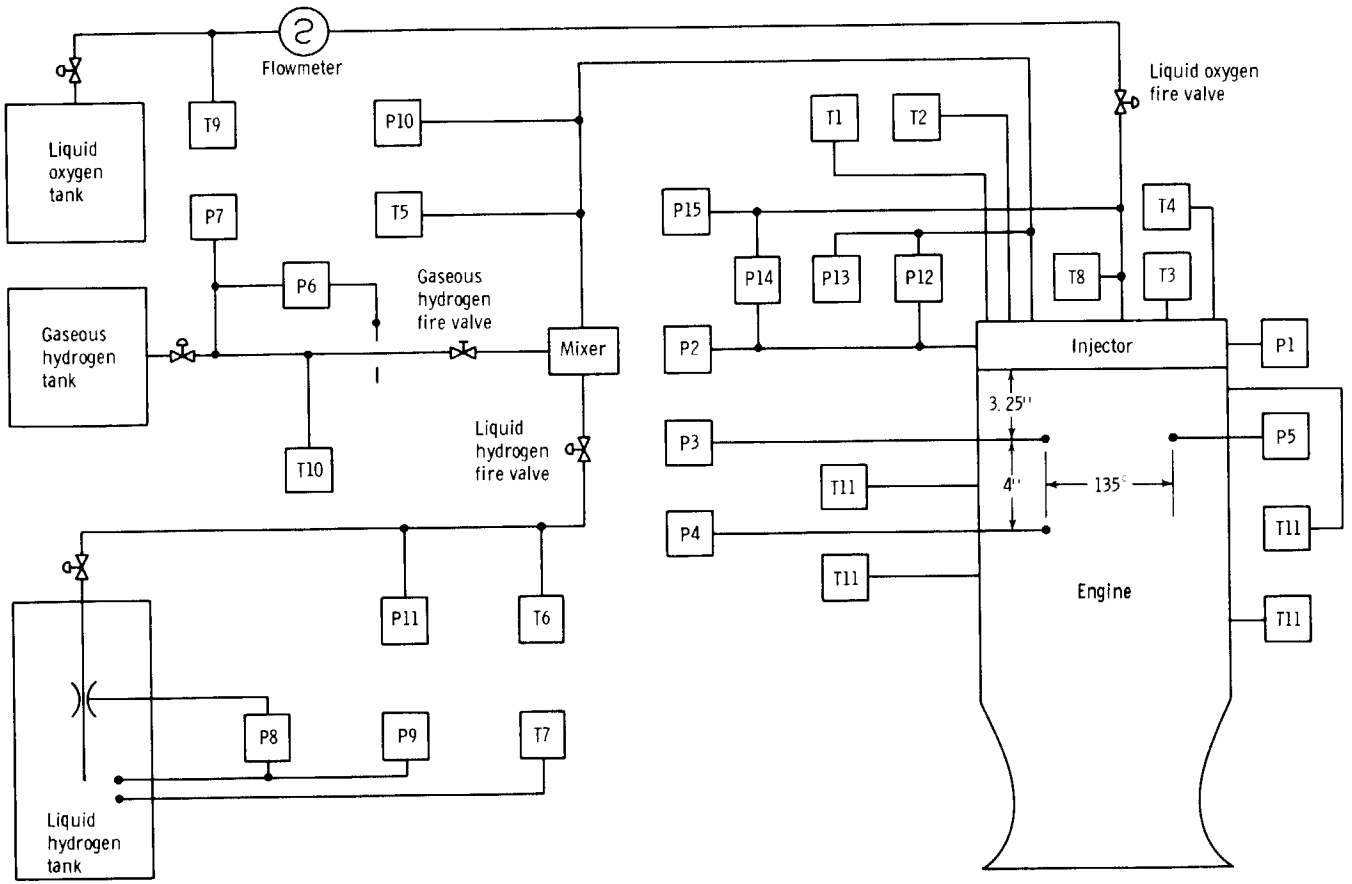

P1 Static chamber pressure (injector face), four-arm strain gage transducer 1
P2 Static chamber pressure (injector face), four-arm strain gage transducer 2
P3 Dynamic chamber pressure, water-cooled quartz pressure transducer 3
P4 Dynamic chamber pressure, water-cooled quartz pressure transducer 4
P5 Dynamic chamber pressure, water-cooled quartz pressure transducer 5
P6 Gaseous hydrogen orifice differential pressure, four-arm strain gage transducer
P7 Gaseous hydrogen orifice pressure, four-arm strain gage transducer
P8 Liquid hydrogen venturi differential pressure, four-arm strain gage type
P9 Liquid hydrogen venturi pressure, four-arm strain gage transducer
P10 Hydrogen mixer pressure, four-arm strain gage transducer
P11 Liquid hydrogen line pressure, four-arm strain gage transducer
P12 Hydrogen injection differential pressure, four-arm strain gage transducer
P13 Hydrogen injection pressure, four-arm strain gage transducer
P14 Oxygen injection differential pressure, four-arm strain gage transducer
P15 Oxygen injection pressure, four-arm strain gage transducer
T1 Hydrogen injector temperature, carbon resistor sensor probe 1
T2 Hydrogen injector temperature, carbon resistor sensor probe 2
T3 Hydrogen injector temperature, carbon resistor sensor probe 3
T4 Hydrogen injector temperature, carbon resistor sensor probe 4
T5 Hydrogen mixer temperature, carbon resistor sensor probe
T6 Liquid hydrogen line temperature, carbon resistor sensor probe
T7 Liquid hydrogen venturi temperature, platinum type
T8 Oxygen injection temperature, copper-constantan thermocouple
T9 Oxygen flowmeter temperature, platinum type
T10 Gaseous hydrogen orifice temperature, iron-constantan thermocouple
T11 Cavity gas temperature, Chromel-Alumel thermocouple (4)

Figure 5. - Instrumentation diagram.

jected hydrogen to a value below the anticipated screech limit. After the first transition point was obtained for a configuration, the ramp rate was reduced in the following runs to minimize mass accumulation in the propellant system and, thus, errors in determination of instantaneous mass flow to the injector. The screech limit was obtained from high-speed recorder data wherein the injector hydrogen temperature in the injector cavity was read at the instant screech was indicated by an oscillograph trace of a flush-mounted pressure transducer. Combustion was considered unstable when a periodic wave-form with an amplitude substantially greater than the normal noise level (10 to 15 psi peak to peak) was observed on the oscillograph record. A typical screech transition is presented in the section RESULTS AND DISCUSSION of the text. Data were obtained over a range of oxidant-fuel ratios to establish a limit curve.

For those configurations that exhibited low screech temperatures below about 70° R, it was necessary to prechill all hydrogen lines and valves down to the fire valve (fig. 5) by a preflow and overboard venting of liquid nitrogen. In addition, still lower temperatures in the 55° to 65° R temperature range required the use of a 1-second lead of liquid hydrogen through the injector for prechill prior to stepping the mixer to the preset condition. Because of the use of heat-sink thrust chambers and nozzles, it was necessary to limit run duration to 3 seconds; accordingly, all valve scheduling was accomplished by the use of an automatic sequence timer.

RESULTS AND DISCUSSION

The investigation reported herein of suppression of high frequency combustion instability using arrays of acoustic damping devices of the Helmholtz type, includes both analytical and experimental results. Theoretical absorption coefficients (fractional part of the energy of an incident sound wave absorbed) are presented to show the effect of variations in liner thickness, backing distance, resonator orifice diameter, open area ratio, and liner cavity gas temperature on damping characteristics. The theory used for liner design is described in the appendix. Experimentally, the effects of changes in these liner design parameters were evaluated during rocket engine firings in terms of self-triggering combustion instability hydrogen injection temperature. The hydrogen temperature rating technique is based on the experience that hydrogen-oxygen combustion can be destabilized by reducing the hydrogen injection temperature. Reference 7 has shown that, basically, the screech stability characteristics are related to propellant injection velocity ratio which is varied with changes in hydrogen temperature. A typical oscillograph trace showing a hydrogen temperature reduction and a transient into screech is presented in figure 6. Screech with a peak-to-peak amplitude of about 150 pounds per square inch was

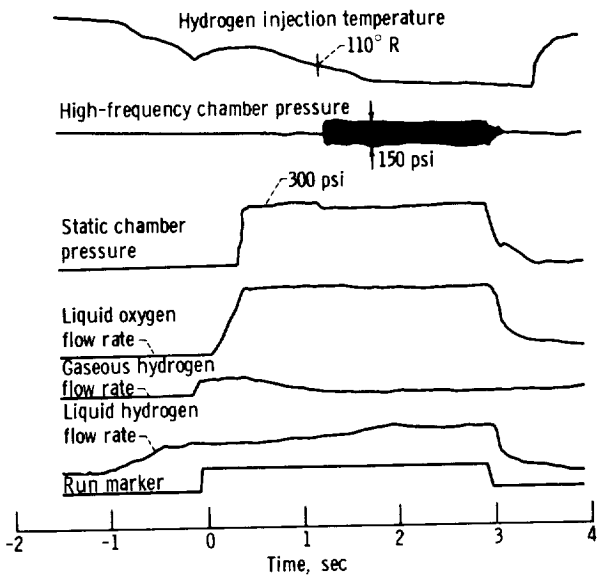

Figure 6. - Oscillograph traces of typical screech test illustrating the temperature rating technique.

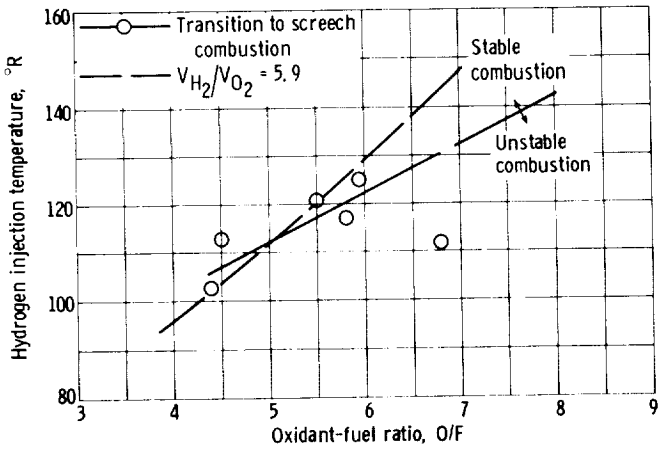

Figure 7. - Hydrogen temperature stable operating limits of engine without liner.

triggered spontaneously when the hydrogen injection temperature reached 110° R with the particular combustor.

Stability Characteristics of Basic Engine

The injector used in the investigation was intentionally selected because of its poor screech stability characteristics, thus, providing a severe test for the liner configurations. The hydrogen temperature stable operating limit as a function of oxidant-fuel ratio is shown for the combustor without liner in figure 7. Each data point represents a separate test, such as the run depicted in figure 6, during which the hydrogen injection temperature was ramped down into screech. The area above the line represents a region of stable operation and, conversely, unstable operation occurs below the line. Similar to the results of reference 7, an oxidant-fuel ratio stability dependence which correlated with a constant injection velocity ratio ($V_{H_2}/V_{O_2} = 5.9$) was observed in the data. The transition temperature increases from a value of 107° R at an oxidant-fuel ratio of 4.5 to 122° R at an oxidant-fuel ratio of 6.

Typical amplitude spectral density graphs of screeching combustion during operation at a hydrogen injection temperature of about 60° R with the basic combustor are presented in figure 8. The predominant mode of instability was first tangential acoustic mode (3000 to 3500 cps). Examination of the graphs shows that the screech amplitude reached values on the order of 140 pounds per square inch peak to peak. In addition to the first tangential mode, large amplitude pressure pulsations were present in several tests at frequencies of 1500, 3800, and 5000 cps. With the exception of the frequency at 3800 cps

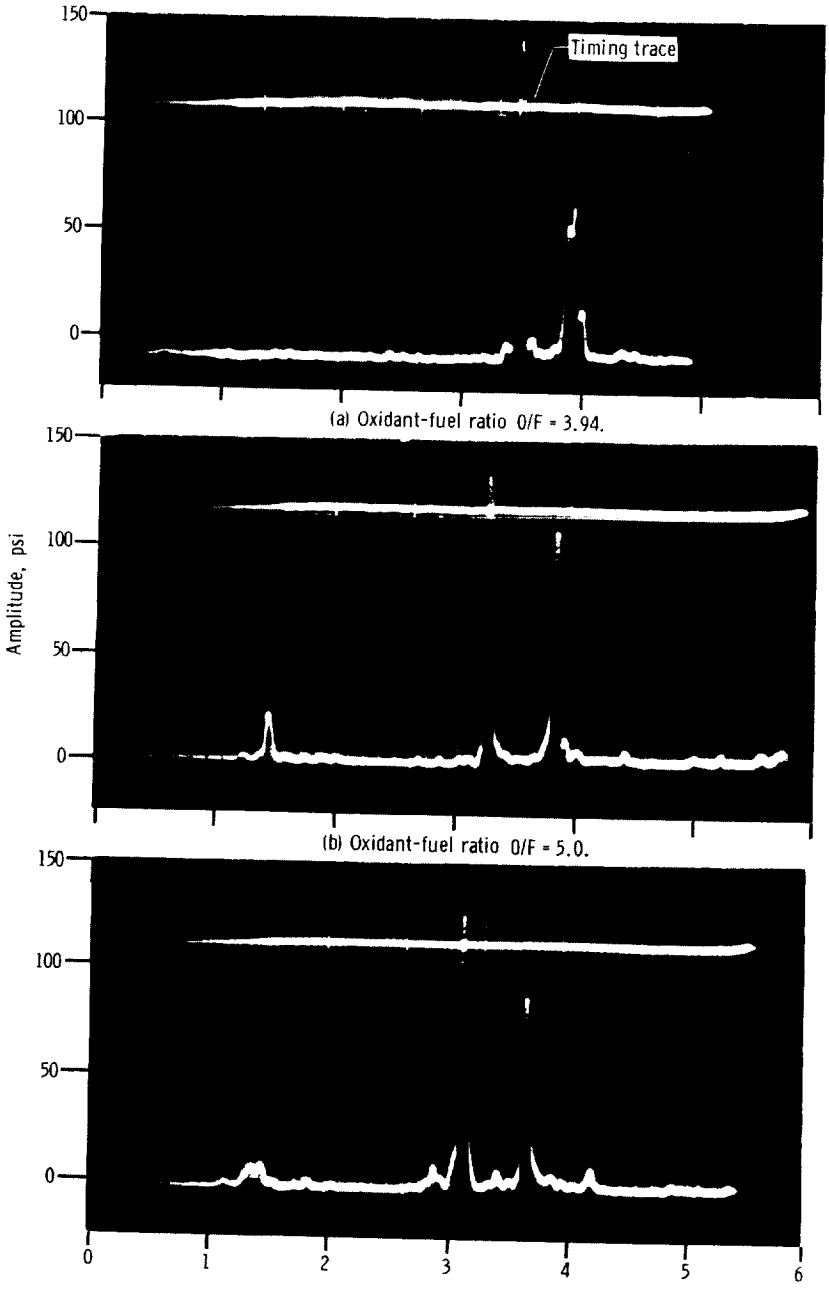

Figure 8. - Typical examples of chamber oscillations during screech at hydrogen injection temperature of 60° R with basic engine.

(second longitudinal acoustic mode), these frequencies do not closely correspond to any common mode. The variations in modal frequencies between tests reflect the change in combustion temperature and, thus, acoustic velocity with oxidant-fuel ratio.

Effect of Resonator Orifice Diameter and Open Area Ratio

In practical liner designs, the wall thickness and, to some degree, backing distance are generally fixed by strength considerations and cooling requirements; thus, the most convenient parameters left to the designer to control acoustic energy absorption are the resonator aperture diameter and the number of resonators. The variation in liner calculated absorption coefficients with open area ratio (total aperture area divided by liner cylindrical surface area) for a range of resonator aperture sizes from 1/8- to 1/2-inch is presented in figure 9. The assumptions made were (1) that the predominant mode of instability was the first transverse mode (3250 cps), (2) that the half amplitude of the incident oscillations was 13 pounds per square inch (an arbitrary value of combustion noise), (3) that the temperature of the gas in the liner cavity was the same as combustion gas temperature (5000° R), and (4) that there was no steady flow past or through the apertures. Gas flow through the apertures was not considered in the design since partitions in the cavity behind the liner (fig. 2, p. 6) were provided to prevent any significant flow behind the liner and, thus, minimize steady or circulatory flow through the apertures. The wall thickness of the liner was 3/4 inch, and the backing distance (annulus height between inner surface of jacket and outer surface of liner) was 0.41 inch. The 3/4-inch wall thickness was a heat-sink requirement (if a 5000° R cavity gas temperature is assumed) for a 3-second-duration run.

As shown in figure 9, the calculated absorption coefficient curves are multivalued;

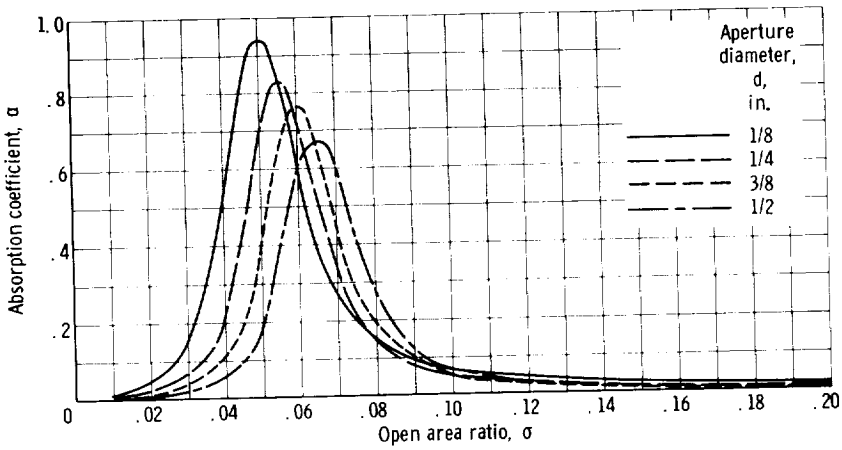

Figure 9. - Calculated absorption coefficient for 3/4-inch-thick wall liner. Liner cavity gas temperature, 5000° R; wave frequency, 3250 cps.

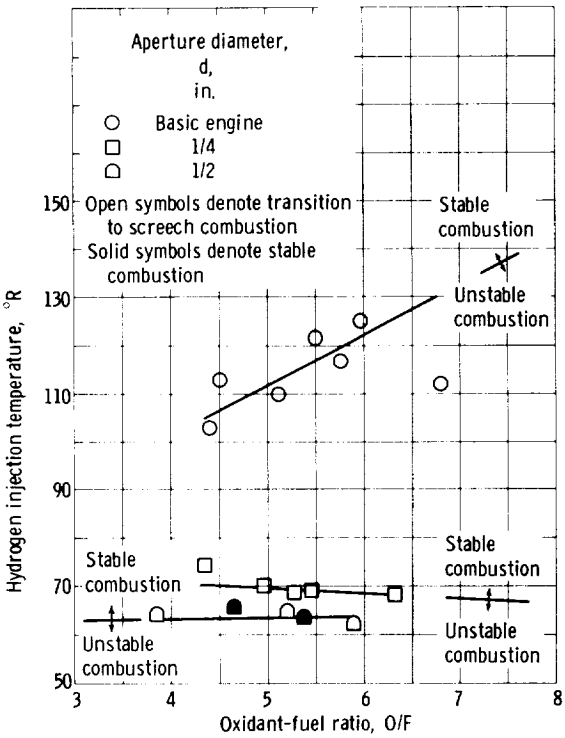

Figure 10. - Hydrogen injector temperature screech characteristics of basic engine and 3/4-inch-thick wall liners.

thus, it is theoretically possible that two liners of different open area ratios could have the same performance. It must be noted here that, although the liner performance is characterized as a function of total area of apertures divided by the total surface area in this figure and others, it actually represents the performance per unit area of the liner. The number of apertures required for screech suppression, and their effectiveness as far as location in the combustor, is discussed in the section Effect of Liner Length. Examination of the figure shows that resonator aperture diameter and open area ratio together affect the liner calculated absorption coefficients. The open area ratio at which optimum liner performance occurs decreases as the aperture diameter decreases. Also, for any aperture size, the number of holes or open area ratio is very critical for good performance. For example, a change in open area ratio from 0.055 to 0.07 decreased the calculated absorption coefficient from 0.83 to 0.34 for 1/4-inch-diameter apertures.

The two 3/4-inch thick liners evaluated experimentally had aperture diameters of 1/4 and 1/2 inch. The resonators had a 1-inch spacing which provided the liners with open area ratios of about 0.05 and 0.2. The hydrogen temperature stable operating limits of the combustor incorporating the 3/4-inch-thick wall liners are compared to the limit of the basic engine in figure 10. Examination of the results of the figure shows that, although the liners did not provide complete screech suppression, a large improvement in the range of hydrogen temperature stable operation was demonstrated. The hydrogen screech transition temperature was about 70° R with the 0.05 open area ratio liner and about 63° R with the 0.2 open area ratio liner compared to 112° R for the basic engine at an oxidant-fuel ratio of 5. The experimental results for the liners are not in agreement with predicted trends (fig. 9); however, as will be shown later, the measured liner cavity gas temperature was different than assumed in the results of figure 9.

The effectiveness of the liners in suppressing the amplitude of screech oscillations at a hydrogen temperature operating condition of 60° R can be seen by comparing the results presented in figures 8, 11, and 12. As would be expected, the liners had the largest effect on the first tangential mode of instability (3000 to 3500 cps). Whereas

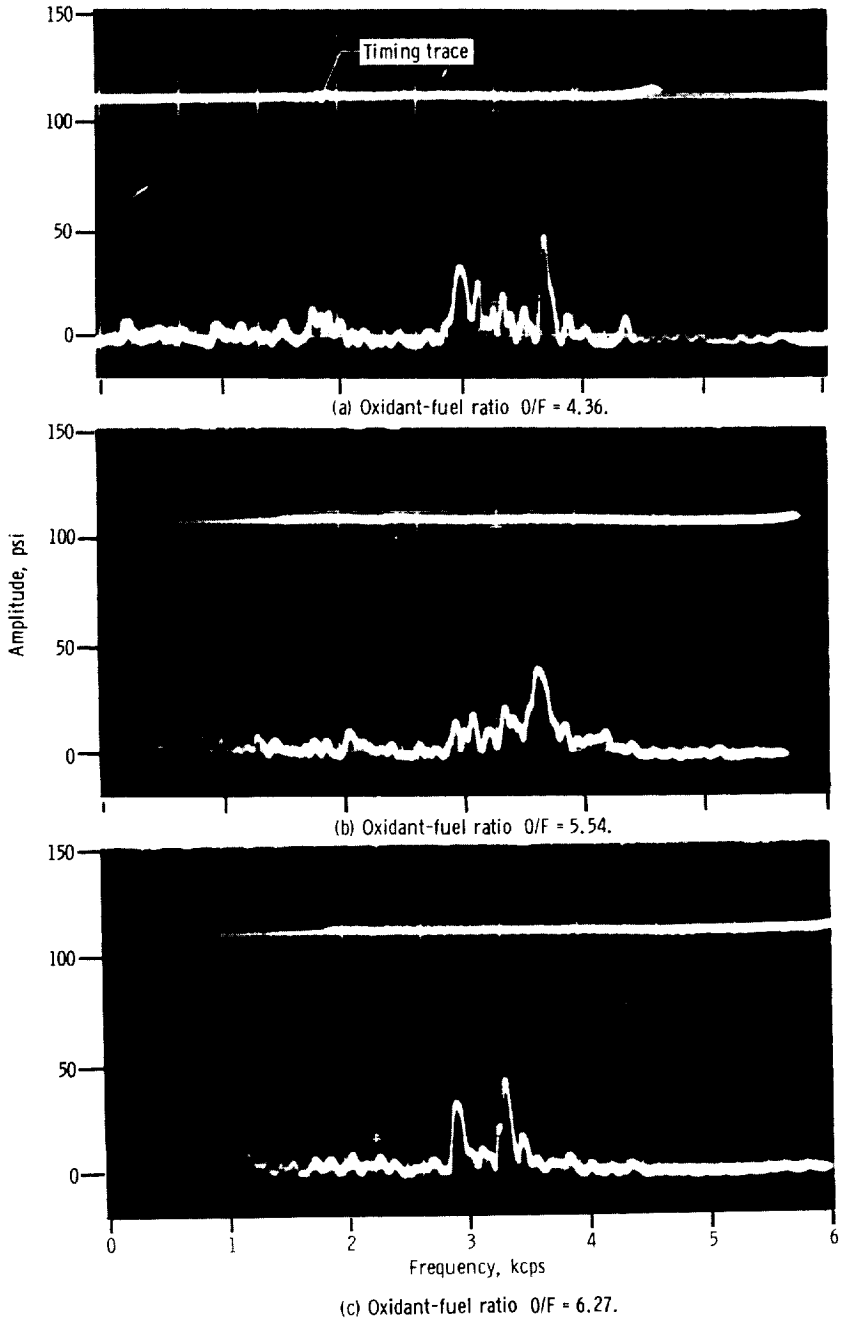

Figure 11. - Typical examples of chamber pressure oscillations during screech at hydrogen injection temperature of 60° R with combustor incorporating 3/4-inch-thick wall, 1/4-inch - diameter apertures, and 0.05 open area ratio liner.

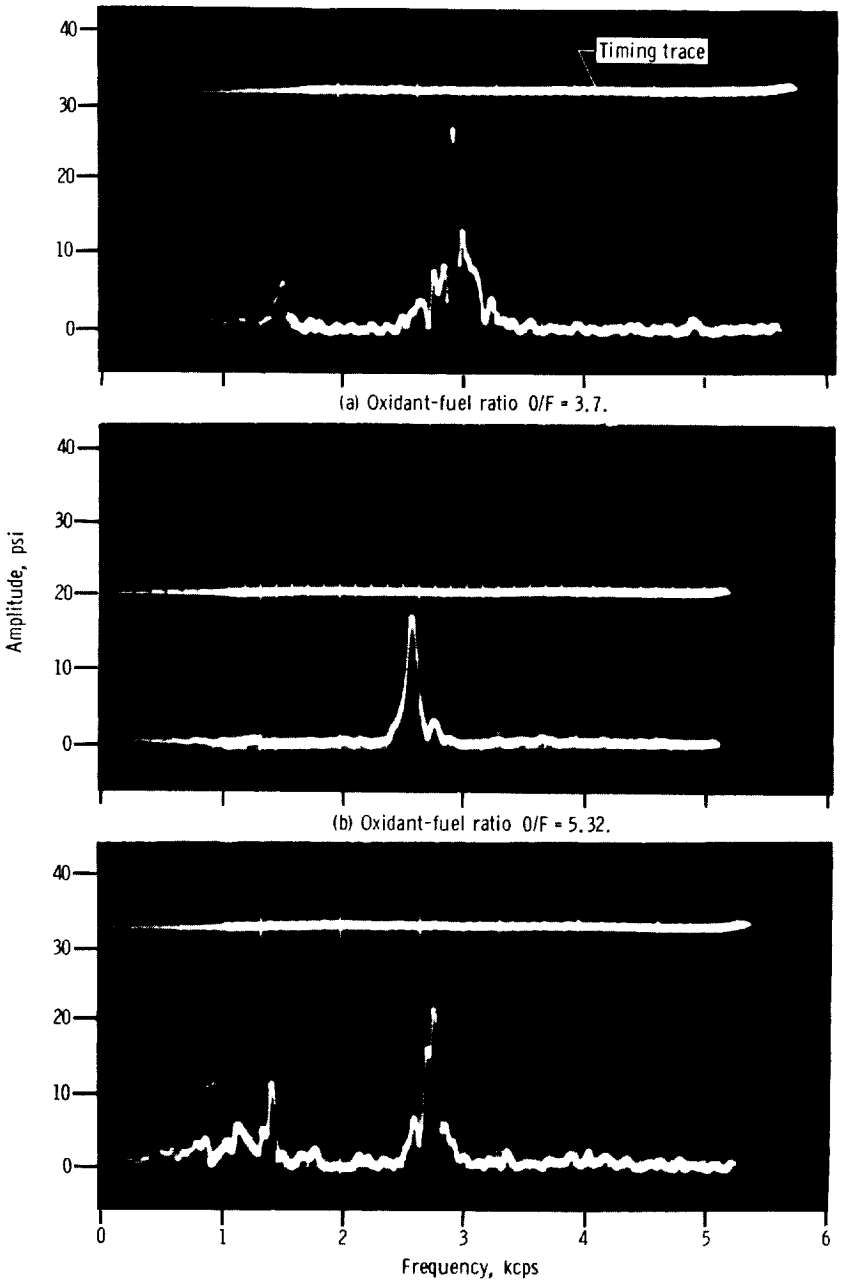

(a) Oxidant-fuel ratio O/F = 3.7.

(b) Oxidant-fuel ratio O/F = 5.32.

(c) Oxidant-fuel ratio O/F = 5.91.

Figure 12. - Typical examples of chamber oxcillations during screech at hydrogen injection temperature of 60° R with combustor incorporating 3/4-inch-thick wall, 1/2-inch-diameter apertures, and 0.2 open area ratio liner.

oscillations with amplitudes of 140 pounds per square inch peak to peak were observed at frequencies between 3000 to 3500 cps with the standard engine, the maximum amplitude observed with the liner was generally less than 30 pounds per square inch in this same frequency range. The amplitude of the second longitudinal mode of instability (3500 to 4000 cps) was also suppressed by the liners, although not to the extent of the tangential mode. When observed, the longitudinal oscillations reach an amplitude of about 40 pounds per square inch compared to 75 pounds per square inch for the basic engine. Reference 1 indicates a shift of the modal frequencies in cold flow tests with perforated liners not exactly tuned to the wave frequency. A pronounced downward frequency shift of the residual tangential mode was observed only with the 0.2 open area ratio liner.

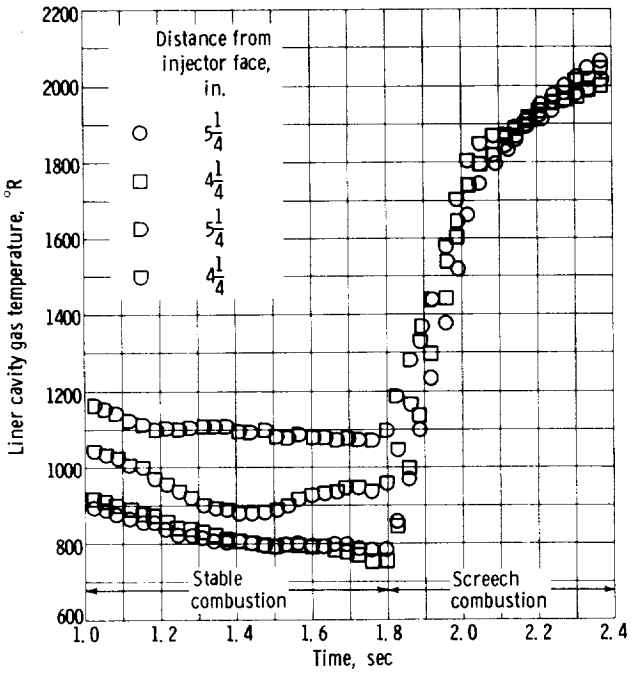

Figure 13. - Typical example of liner cavity gas temperature during stable and unstable combustion with combustor incorporating 3/4-inch-thick wall, 1/4-inch-diameter aperture, and 0.05 open area ratio liner.

A typical time history of the gas temperature behind the 0.05 open area ratio liner is shown in figure 13. The level of the cavity gas temperature during the run was very much lower than the assumed value of 5000° R. Prior to inception of screech, the gas temperature measured in four locations behind the liner varied between 800° and 1100° R. At about 1.8 seconds when screech was encountered, the temperature of the gas in the liner cavity rapidly increased to a value of about 2000° R, however, still considerably lower than the value assumed in the liner design.

The theoretical absorption character-

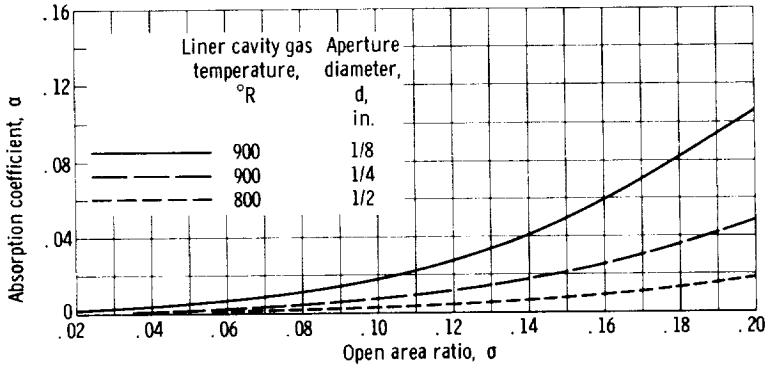

Figure 14. - Calculated absorption coefficient for 3/4-inch-thick wall liners. Wave frequency, 3250 cps.

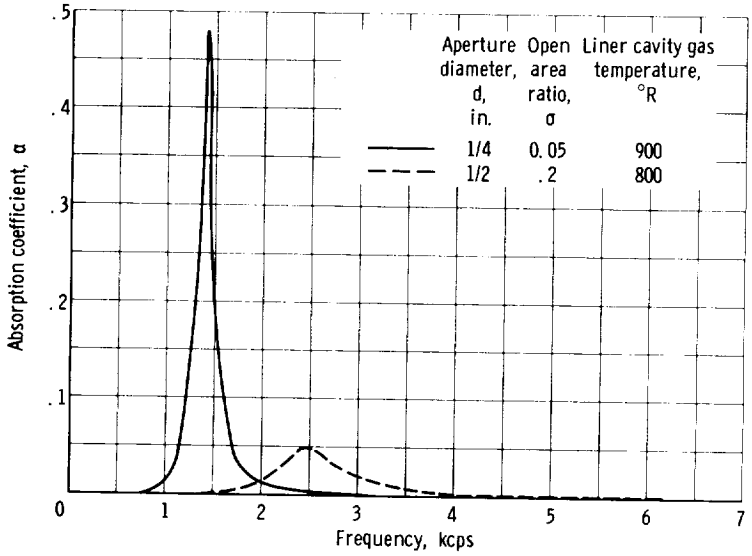

Figure 15. - Absorption frequency bandwidth of 3/4-inch-thick wall liners.

istics of the liners were reevaluated at an average liner cavity gas temperature typical of the values measured just prior to screech inception (other design inputs same as before). The calculated absorption coefficients are presented in figure 14 as functions of the open area ratio. Examination of the figure shows a drastic reduction in absorption coefficient of the 3/4-inch wall thickness liner and a pronounced aperture diameter effect at the lower cavity gas temperature (in comparison to fig. 9). For example, the calculated absorption coefficient of the 0.05 open area ratio liner configuration at a wave frequency of 3250 cps was only on the order of 0.005. These results also indicate that the open area ratio must be increased and the aperture diameter decreased to improve the performance of the 3/4-inch wall liners at the low cavity gas temperatures. The cavity resonant frequency (frequency at which absorption maximizes) for both designs was lower than the first transverse mode of about 3250 cps at the low cavity gas temperatures measured prior to screech inception (fig. 15). At a frequency of 3250 cps, the liner configuration with 1/2-inch apertures which had the best hydrogen temperature stable operating range (fig. 10), also had the highest calculated absorption coefficient of 0.018. The calculated absorption coefficient of the 0.05 open area liner which lowered the screech transition temperature by 42° R had a calculated absorption coefficient of less than 0.005 at 3250 cps.

Effect of Liner Thickness and Backing Distance

The results of the previous section indicate that complete suppression of screech at very low hydrogen injection temperatures (60° R) could probably be accomplished with liners for which relatively low values of energy absorption were calculated. Although the absorption coefficient of the 3/4-inch-thick wall liners could be increased by decreasing

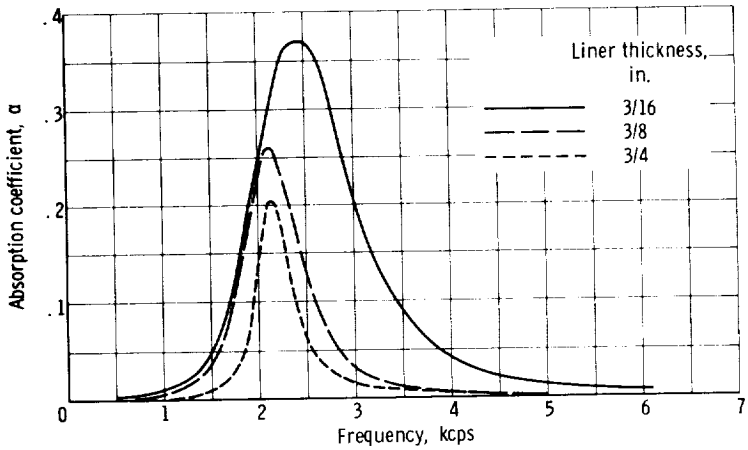

Figure 16. - Effect of liner thickness on absorption frequency bandwidth. Aperture diameter, 1/4 inch; open area ratio, 0.1; liner cavity gas temperature, 1000° R.

the resonator aperture diameter and adjusting open area ratio (fig. 14), the heavy-wall, heat-sink liner was not considered practical geometry for application to a flight-weight design; thus, no further attempt was made to improve its performance. An alternate method to provide a liner with better absorption characteristics at the low cavity gas temperatures and without changing the diameter of the thrust chamber jacket was to decrease the liner wall thickness while simultaneously increasing the backing distance. From a structural standpoint, decreasing wall thickness was considered possible because the cavity gas temperature was very much lower than assumed in the original design (5000° R).

A comparison of the theoretical absorption characteristics of liners with wall thicknesses of 3/4, 3/8, and 3/16 inch is presented in figure 16. The inner jacket internal dimension was held constant for all configurations; thus, the backing distance varied from 0.41 inch for the 3/4-inch-thick wall, to 0.785 inch for the 3/8-inch-thick wall, and to 0.9745 inch for the 3/16-inch-thick wall liner. Calculated absorption coefficients are presented as a function of frequency for liners with 1/4-inch-diameter apertures at a liner cavity gas temperature of 1000° R and no steady flow past the apertures. Examination of the figure shows that the damping characteristics can be significantly improved by reducing the wall thickness and correspondingly increasing the backing distance. For example, decreasing the wall thickness from 3/4 to 3/16 inch while increasing the backing distance from 0.41 to 0.9745 inch, increases the theoretical absorption coefficient from about 0.01 to 0.13 at a frequency of 3250 cps. In addition to providing improved damping, the thin wall liner design also improves the absorption frequency bandwidth. At half power level, the absorption frequency bandwidth was increased by about a factor of 2 by decreasing the wall thickness from 3/4 to 3/16 inch.

In an attempt to verify these analytical results, an existing 3/4-inch-thick wall copper liner was machined down to a wall thickness of 3/8 inch. The aperture diameter was 1/8 inch, and the open area ratio was 0.1. Screech was encountered at a hydrogen

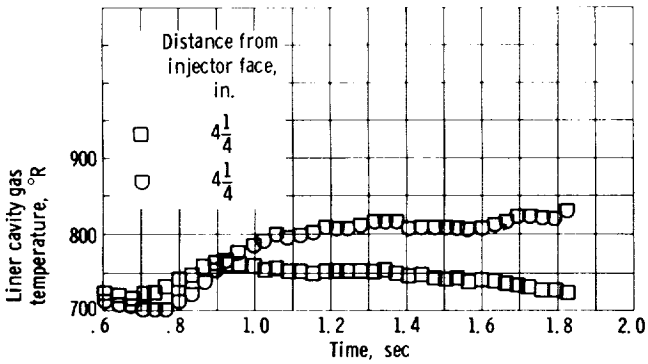

Figure 17. - Typical example of cavity gas temperature during stable combustion with combustor incorporating 3/16-inch-thick wall, 1/4-inch-diameter aperture, and 0.1 open area ratio liner.

temperature of about 65° R in three of the five tests of this liner. The measured cavity gas temperature for this liner immediately prior to screech was 600° R, lower than the values measured with the 3/4-inch wall configurations. At this cavity temperature, the absorption coefficient for the 3/8-inch wall liner was calculated to be 0.019, approximately the same as the 3/4-inch wall liner with 1/2-inch apertures. The improvement in stable operating limits provided by the two different wall thickness liners was also the same, which lends confidence to use of acoustic theory in liner design.

A further reduction in liner wall thickness to 3/16 inch improved the hydrogen temperature stable operating limits as predicted by theory. A 3/16-inch wall thickness, 0.1 open area ratio liner with 1/4-inch apertures provided stable operation at 60° R, the minimum temperature attainable in the facility. Calculating the liner absorption coefficient at a measured cavity gas temperature of 800° R (fig. 17) produced a coefficient of 0.055.

Typical examples of amplitude spectral density graph of combustion pressure oscillations during operation at hydrogen temperatures of about 60° R with the 3/8- and 3/16-inch liners are presented in figures 18 and 19. The mode of instability encountered with the 3/8-inch wall thickness liner was complex (fig. 18), containing a maximum pressure amplitude of 40 pounds per square inch at about 3100 cps (first tangential mode) and several lesser spikes at frequencies between 2600 and 3500 cps. In addition, pronounced pressure amplitudes were present at 1500 and 5200 cps (second tangential mode). The maximum pressure amplitude in the screech frequency range observed during tests of the 3/16-inch-thick wall liner was on the order of 10 to 15 pounds per square inch (fig. 19). The low to intermediate frequencies (0 to 1000 cps) which could possibly be entropy waves (ref. 10) were not eliminated by the liner.

Effect of Open Area Ratio and Liner Cavity Temperature

The analysis and design of absorbing liners for rocket engines is complicated by the variance in liner cavity gas temperatures between liner configurations. Typical values of gas temperature behind the liner with changes in open area ratio from 0.05 to 0.2 for

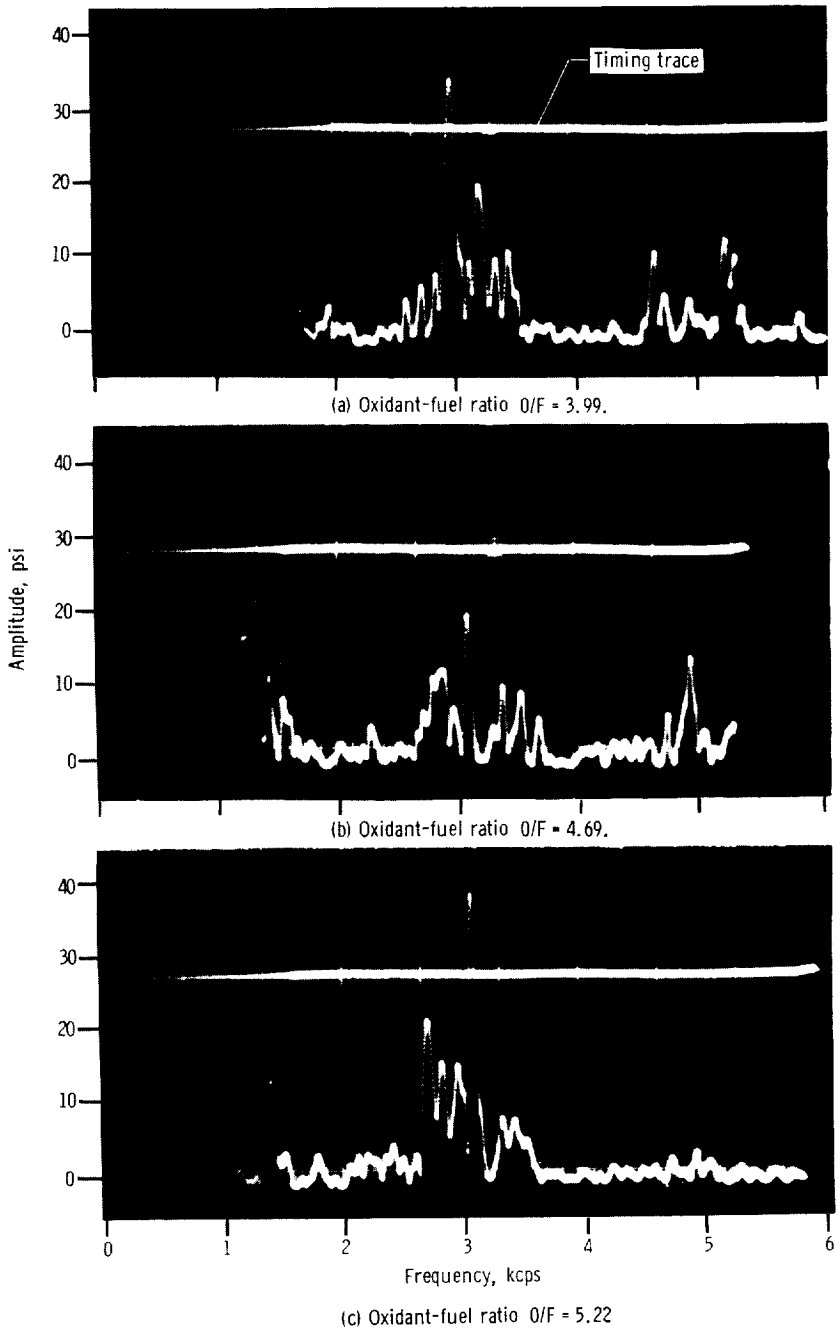

Figure 18. - Typical examples of chamber pressure oscillations during operation at hydrogen temperature of 60° R with combustor incorporating 3/8-inch-thick wall, 1/8-inch-diameter apertures, and 0.1 open area ratio liner.

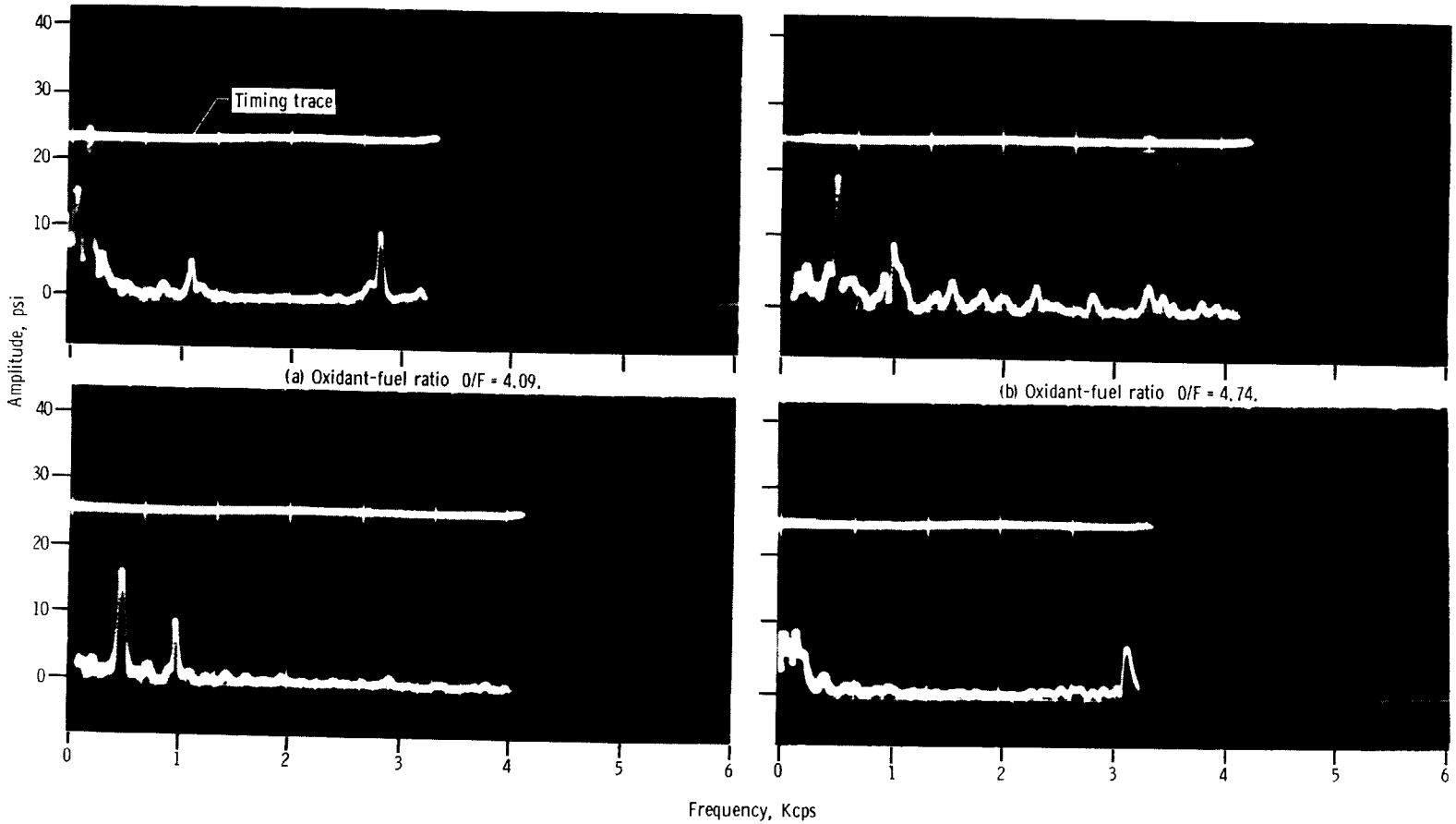

Figure 19. - Typical examples of chamber pressure oscillations during operation at hydrogen injection temperature of 60° R with combustor incorporating 3/16-inch-thick wall, 1/4-inch-diameter apertures, and 0.1 open area ratio liner.

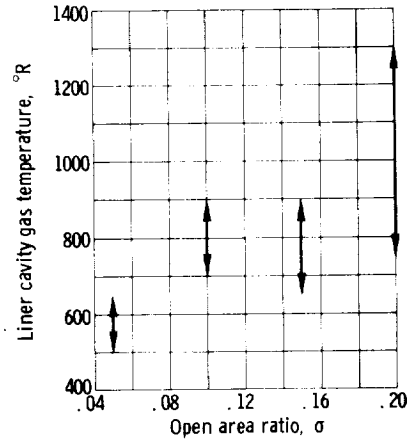

Figure 20. - Effect of open area ratio on liner cavity gas temperature. Liner wall thickness, 3/16 inch; aperture diameter, 1/4 inch; oxidant-fuel ratio O/F ≃ 5.

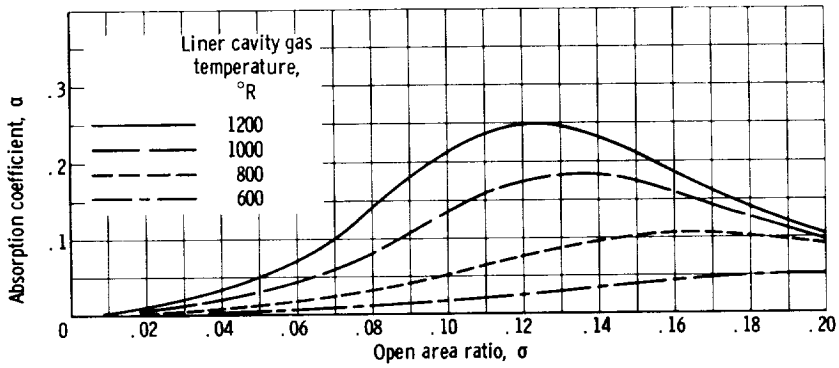

Figure 21. - Effect of liner cavity gas temperature on calculated absorption coefficient of 3/16-inch-thick wall liner with 1/4-inch-diameter apertures. Wave frequency, 3250 cps.

a constant aperture diameter of 1/4 inch are shown in figure 20. The results show that the gas temperature behind the 3/16-inch-thick wall liner varied between 500° and 650° R at an open area ratio of 0.05 (prior to inception of screech) depending on the axial location. As would be expected, the liner cavity gas temperature also varied with the number of apertures per unit area. The cavity gas temperature (average) increased from 600° R at an open area ratio of 0.05 to 1000° R at an open area ratio of 0.2. This variance in gas temperature undoubtedly results from the different amount of combustion gas recirculation under the liner. In addition, a variation in cavity gas temperature with injector element size and spacing and also the propellant combination, along with the amount of film cooling employed, might also be expected. Thus, unless a means of controlling liner cavity gas temperature is found, such as a gas bleed, the designer is faced with an experimental program to optimize the final acoustic liner design.

The effect of cavity gas temperature on the theoretical absorption characteristics of a 3/16-inch-thick wall liner with 1/4-inch apertures is shown in figure 21. Computed absorption coefficients are presented as functions of open area ratio for a range of liner cavity gas temperatures from 600° to 1200° R. For a 0.1 open area ratio liner, a decrease in liner cavity gas temperature from 1200° to 600° R decreased the calculated absorption coefficient from about 0.21 to 0.02 at a frequency of 3250 cps. The effect of the temperature is to change the tuning or the resonant frequency of the cavity, thus, changing the absorption characteristics of the resonator. It must be noted that these results do not preclude the use of cold gas to control cavity gas temperature. For example, the absorption coefficient of a 3/16-inch wall, 0.1 open area ratio liner with a backing distance of $1\frac{3}{4}$ inches was calculated to be 0.42 with an ambient hydrogen environment (520° R) in the cavity behind the liner.

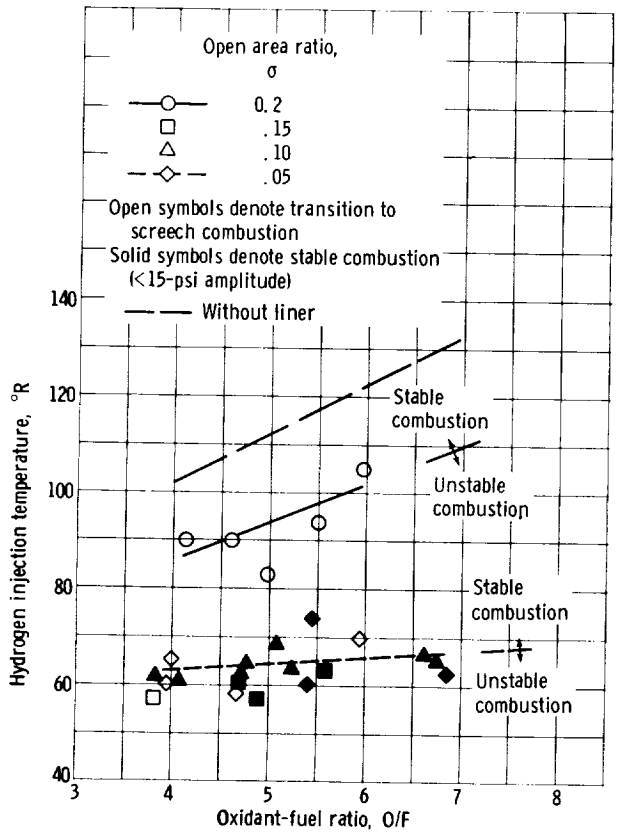

Figure 22. - Hydrogen temperature stable operating limits of various open area ratio, 3/16-inch-thick wall liners. Aperture diameter, 1/4 inch.

The hydrogen temperature stable operating limits for the 3/16-inch wall thickness liner configurations are presented in figure 22 as a function of oxidant-fuel ratio. As shown in the figure, screech was encountered with the 0.05 and 0.2 open area ratio liners while the 0.1 and 0.15 open area ratio configurations provided stable combustion at a hydrogen injection temperature of 60° R. The peak-to-peak amplitude of chamber pressure oscillation at a frequency corresponding to the first tangential mode was generally less than 10 pounds per square inch (figs. 19 and 23) for the stable combustor configurations. The 0.05 and 0.2 open area ratio liners had a screech amplitude of about 35 pounds per square inch (fig. 24) and about 25 pounds per square inch (fig. 25), respectively, at a 60° R hydrogen temperature operating condition. The calculated absorption coefficients for the 3/16-inch-thick wall liner configurations, which were computed at the measured values of cavity gas temperature (fig. 20), are presented in figure 26 as functions of wave frequency. The variation in stable operating limits with the calculated absorption coefficients at a wave frequency of 3250 cps (first tangential acoustic mode) is shown in figure 27. An anomaly exists between theoretical predictions and the experimental results when the calculations include the assumption of no flow past the apertures. Two configurations (0.2 and 0.15 open area ratio) with the same calculated absorption coeffi-

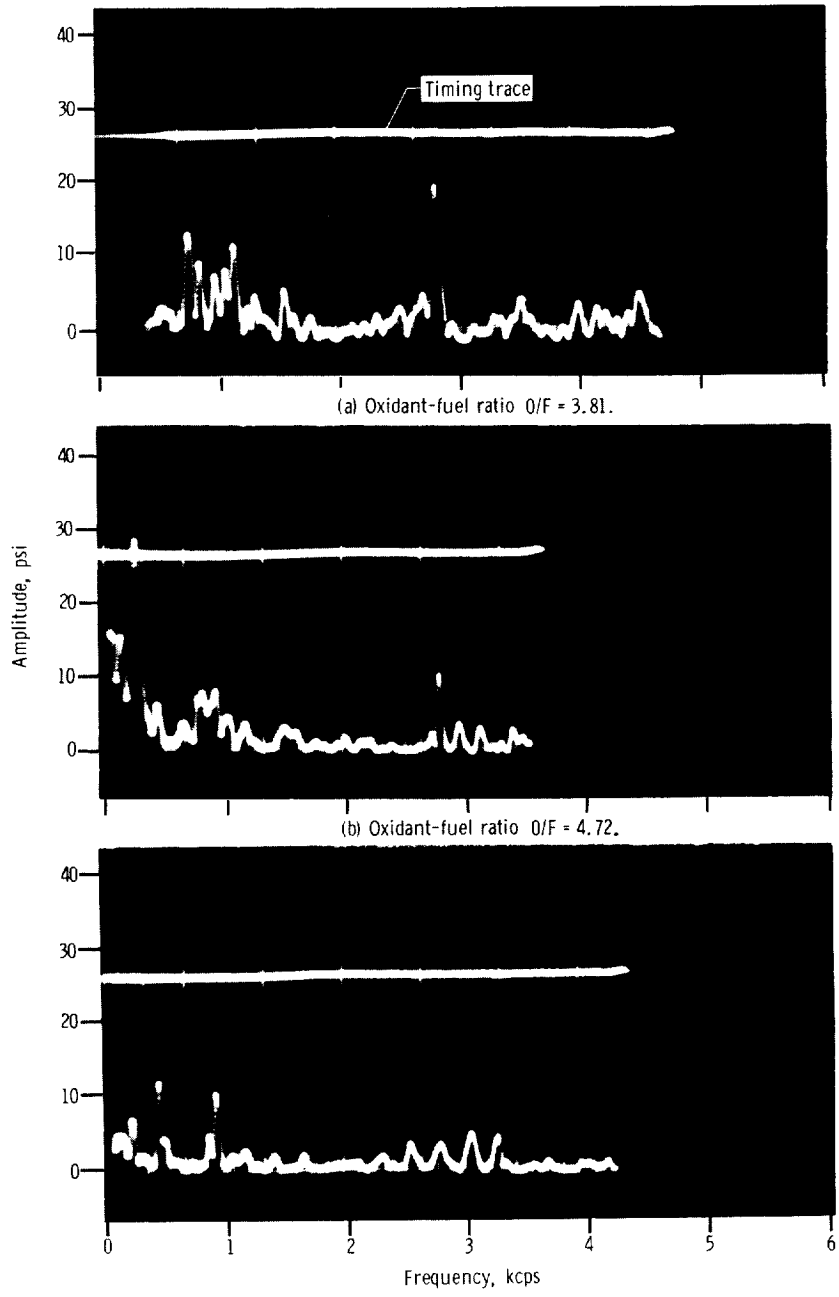

(a) Oxidant-fuel ratio O/F = 3.81.

(b) Oxidant-fuel ratio O/F = 4.72.

(c) Oxidant-fuel ratio O/F = 5.6.

Figure 23. - Typical examples of chamber pressure oscillations during operation at hydrogen injection temperature of 60° R with combustor incorporating 3/16-inch-thick wall, 1/4-inch-diameter apertures, and 0.15 open area ratio liner.

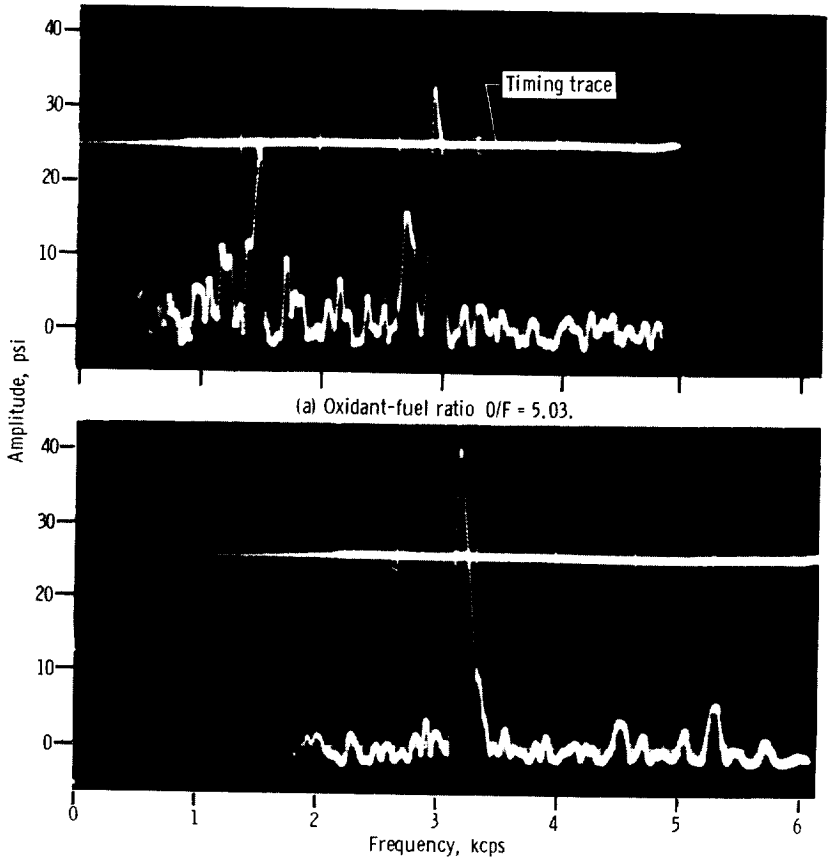

(b) Oxidant-fuel ratio O/F = 3.95.

Figure 24. - Typical examples of chamber pressure oscillations during screech at hydrogen injection temperature of 60° R with combustor incorporating 3/16-inch-thick wall, 1/4-inch-diameter apertures, and 0.05 open area ratio liner.

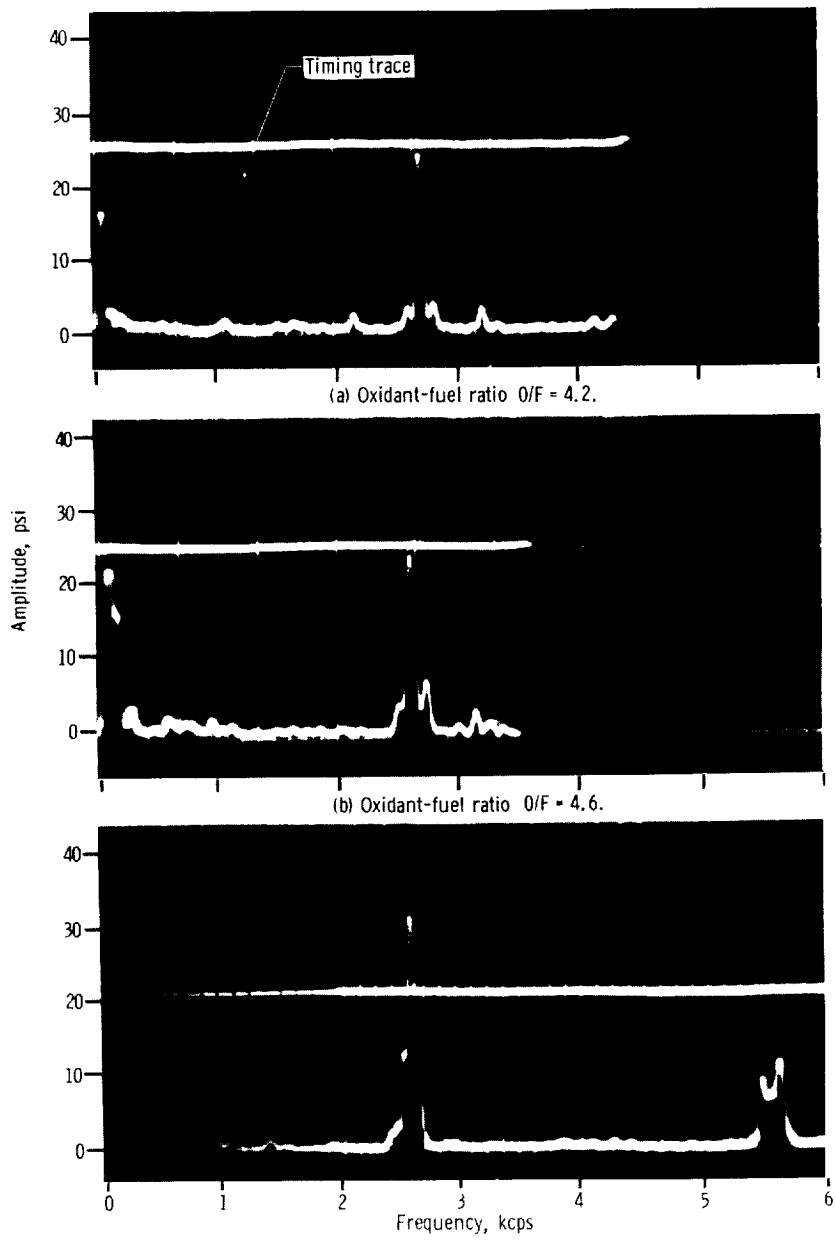

(a) Oxidant-fuel ratio O/F = 4.2.

(b) Oxidant-fuel ratio O/F = 4.6.

(c) Oxidant-fuel ratio O/F = 5.45.

Figure 25. - Typical examples of chamber pressure oscillations during operation at hydrogen temperature of 60° R with combustor incorporating 3/16-inch-thick wall, 1/4-inch-diameter apertures, and 0.2 open area ratio liner.

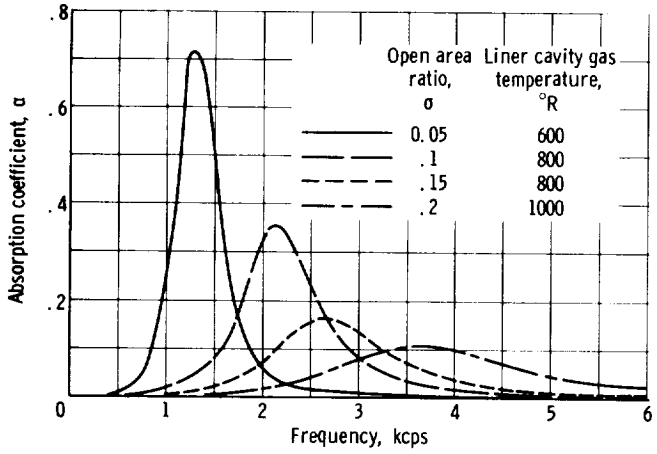

Figure 26. - Frequency absorption bandwidth of various 3/16-inch-thick wall liners with 1/4-inch-diameter apertures.

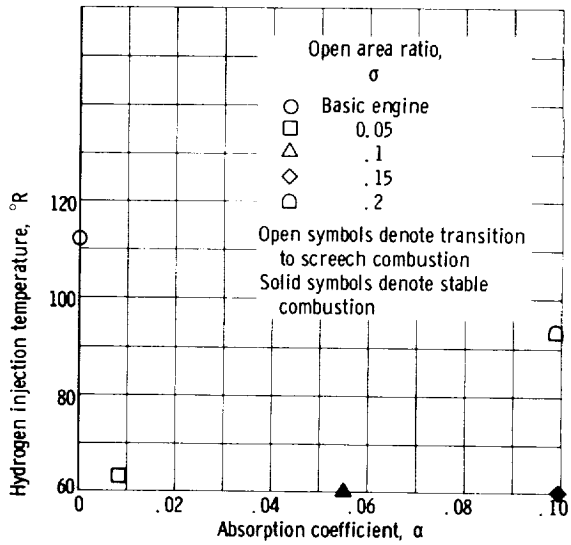

Figure 27. - Variation of hydrogen temperature stable operating limits with calculated liner absorption coefficient for 3/16-inch-thick wall full length liner without effects of flow past.

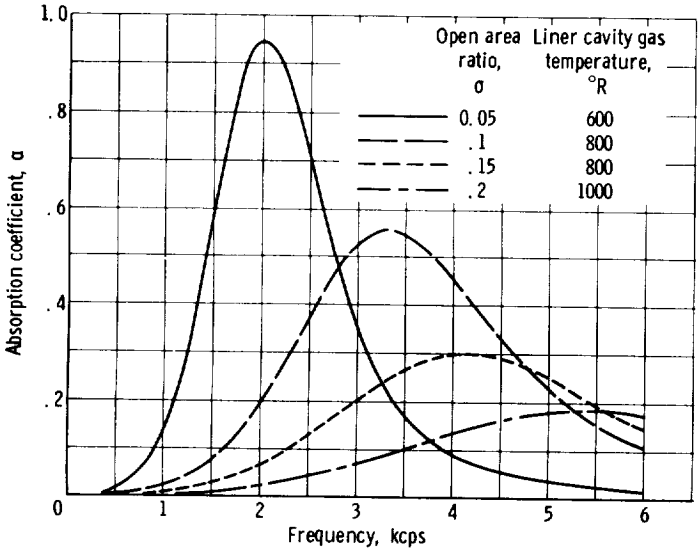

Figure 28. - Frequency absorption bandwidth of 3/16-inch-thick wall liners with 1/4-inch-diameter apertures. Velocity past apertures, 280 feet per second.

cient of 0.099 at a frequency of 3250 cps provided different hydrogen temperature stable operating conditions. In view of this disagreement of the predicted trends and experimental data, the original design assumptions were modified to include the effects of side velocity or flow past the apertures. The effective length, or mass, of the vibrating slug in the resonator neck is reduced by increasing side velocity, thus changing the tuning, or the resonant frequency, of the spring-mass system. Since the velocity of the flow past the apertures was not known, a trial and error process was used to arrive at a velocity that would best fit the experimental results from the viewpoint of absorption. The absorption frequency bandwidth of the liners with a 280-foot-per-second side velocity is presented in figure 28. As

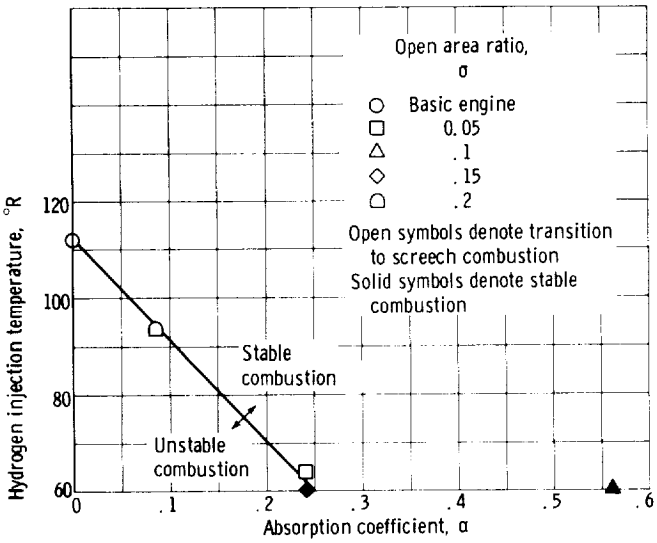

Figure 29. - Variation of hydrogen temperature stable operating limits with calculated absorption coefficient for 3/16-inch-thick wall, full length liners. Side velocity, 280 feet per second.

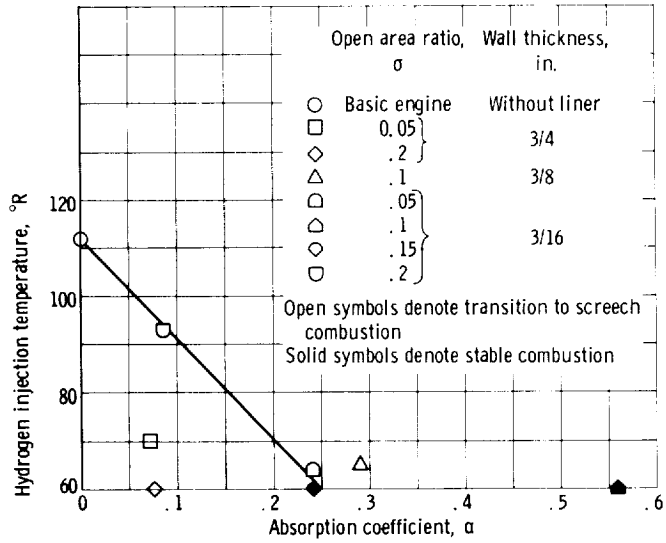

Figure 30. - Variation of hydrogen temperature stable operating limits with calculated liner absorption coefficients for all full length liners. Side velocity, 280 feet per second.

can be seen in figure 29, a better agreement between experimental data and predicted trends was obtained when the effects of a 280-foot-per-second side velocity (about 0.2 free stream velocity) were included in the calculations. This correlation indicates that a liner with a minimum absorption coefficient of about 0.25 would be required to stabilize combustion at a hydrogen injection temperature of 60° R for the particular injector used in this investigation. The magnitude of the side velocity for best correlation suggests that it represents a flow past the first few rows of resonators from the injector which, as will be discussed in the section Effect of Liner Length, contribute most to the stability of the combustor.

The results of all liner configurations presented in the previous figures are summarized in figure 30. A satisfactory agreement between the thick wall and thin wall configurations was not obtained even when the effects of a 280-foot-per-second side velocity were included in calculations of liner absorption coefficient. Possibly, the effects of side velocity may change with aperture diameter and liner wall thickness. Additional data would be required to conclusively evaluate these effects.

It must be noted that the previous correlation was based on a wave frequency of 3250 cps, typical of the first transverse mode of instability observed in the basic engine without an acoustic liner (fig. 8, p. 13). Correlating the

results on the shifted frequency observed in tests with liners (generally less than 3250 cps) lowered the side velocity from 280 to 240 feet per second at which the best agreement between theory and experiment was attained. A side velocity of 240 feet per second, however, did not improve the agreement between thick and thin wall liners.

Effect of Liner Length

Combustion instability in rocket engines has been successfully suppressed in many instances by the use of injector face baffles (ref. 11). Successful baffles have varied greatly in length from one engine to another; however, in all cases, the baffle lengths were short compared to the length of the thrust chamber. Thus, it was hypothesized that damping need only be provided near the injector end of the thrust chamber, possibly at the point of highest energy release, to suppress combustion instability. The effect of length was experimentally evaluated with a 0.1 open area ratio, 3/16-inch wall liner, the most successful full length configuration. Liner length variations included were 17, 34, and 50 percent of the full length configuration. The partial length configurations were evaluated positioned only at the injector end of the thrust chamber.

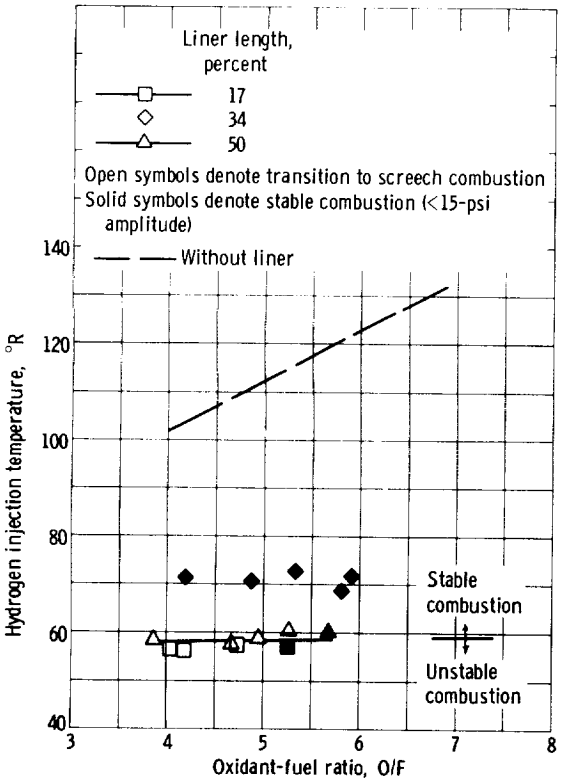

Figure 31. - Effect of liner length on hydrogen temperature stable operating limits. Wall thickness, 3/16 inch; aperture diameter, 1/4 inch.

The hydrogen temperature stable operating limits of the combustor incorporating the various length liner configurations are presented in figure 31. The stable operating limits of the 17 and 50 percent partial length liner configurations were the same, with transitions into screech at a hydrogen temperature of about 58° R. The operating limit was not defined for the 34 percent partial length configuration because of a facility limitation at the time of the tests. Screech was not encountered during the full length liner tests (fig. 22, p. 25); however, the configuration was not evaluated at as low a hydrogen temperature as the partial length configurations. The instability (first tangential mode) encountered with the partial length configurations was not a sustained type, but one consisting of short bursts of 0.1 to 0.2 second in duration. The maximum peak-

to-peak screech amplitude measured was about 50 pounds per square inch. Although not conclusively evaluated, it appears from these results that full combustion length liners are not required for screech suppression. The sensitive area appears to be the first few inches from the injector face. Undoubtedly, the length of liner required for screech suppression will vary with engine size, thrust per element, and the propellant combination.

Effect of Filling the Liner Cavity with Porous Material

One limitation of simple perforated plate acoustic liners, especially at low frequencies, is that such liners absorb selectively in the region of resonance only. Several techniques, however, can be employed to alter the absorption frequency bandwidth of a liner, one of which is to fill the liner cavity with a porous material (ref. 12). Porous material in the liner cavity increases the specific acoustic resistance which extends the frequency range of absorption and simultaneously, it increases the absorption coefficient providing the specific acoustic resistance θ is less than one. Referring to equation (A1) (see appendix) reveals that α is a maximum when θ equals one.

The effect of filling the resonator volume with porous material was evaluated using a 0.2 open area ratio, 3/16-inch wall thickness liner, the configuration that provided the least improvement in hydrogen temperature operating limits. The screech transition temperature for this configuration (unfilled) was 93° R at an oxidant fuel ratio of 5. The material used to fill the liner cavity was grade 2-medium steel wool packed to a density of 0.014 pounds per cubic inch. Examination of the results presented in figure 32 shows a marked improvement in stability with the steel wool filled liner. The filled configuration provided stable operation at a hydrogen injection temperature of about 58° R (minimum available in the facility).

No attempt was made to calculate a theoretical absorption coefficient for the filled liner because adequate data on porosity and structure factor of the porous material were not available. However, inasmuch as complete stabilization was achieved, the adsorption coefficient of the liner must have increased to a value greater than 0.25 (minimum value of the coefficient for stable operation at 60° R obtained from the correlation in fig. 29, p. 30). The maximum adsorption coefficient for this configuration (unfilled) was about 0.19 (fig. 28, p. 29).

It must be noted, however, that the use of steel wool as a liner cavity fill material would not be suitable (without some method of cooling) for long duration operation inasmuch as burning occurred in the upstream portion (fig. 33) during the tests with a total duration of about 11 seconds.

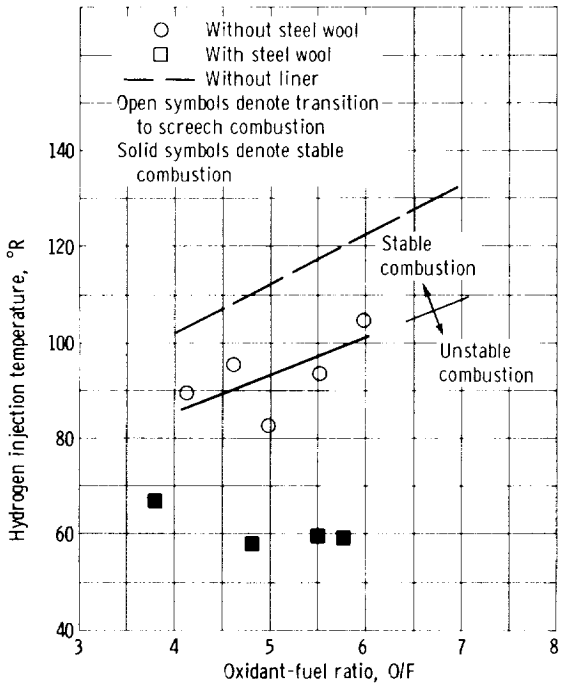

Figure 32. - The effect of packing the resonator volume of an 0.2 open area, 3/16-inch-thick wall liner with steel wool.

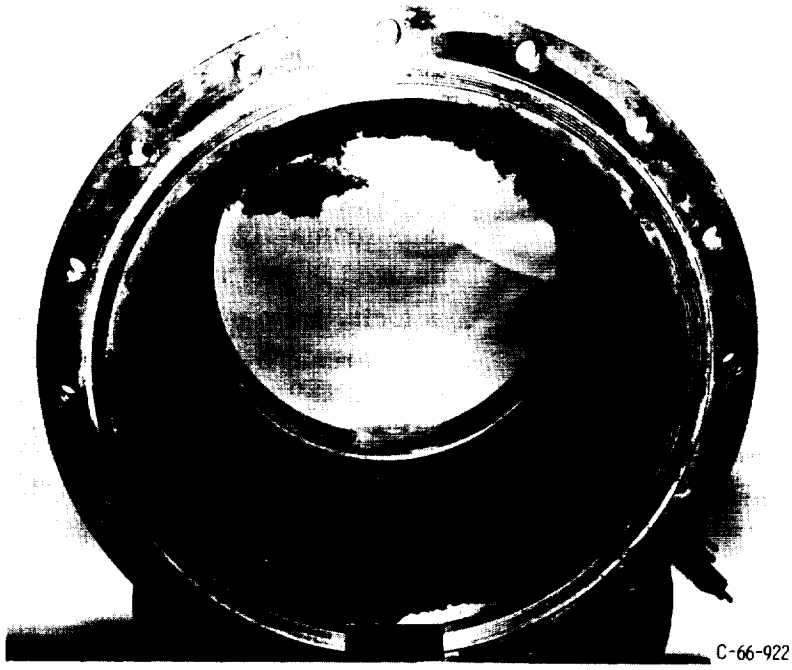

Figure 33. - Postfire condition of steel wool packing in liner cavity.

Engine Performance

Although good combustion efficiency was not a primary consideration in the design of the injector that was used in this investigation, its characteristic exhaust velocity efficiency of 97 percent at an oxidant-fuel ratio of 5 compares favorably with the state of the art. Variation of engine performance with oxidant-fuel ratio during stable combustion at a hydrogen injection temperature of 120° R is presented in figure 34. Performance dropped off slightly as oxidant-fuel ratio was increased. Also included on the figure are performance data of the engine with acoustic liners. Liners had no apparent effect on engine performance at this hydrogen temperature operating condition. Figure 35 presents the performance of the combustion during stable operation at a hydrogen injection temperature of 60° R. The characteristic exhaust velocity efficiency decreased to about $92\frac{1}{2}$ percent at an oxidant-fuel ratio of 5. The decay of performance at low hydrogen injection temperatures is not believed to be a temperature effect but rather its influence on hydrogen injection velocity through changes in the propellant density. Evidence to support this concept of hydrogen injection velocity can be found in reference 7 which develops a correlation of hydrogen stable operating limits with a constant injection velocity ratio irrespective of the level of hydrogen temperature. Combustion performance for this referenced series of concentric tube injectors (approximately the same number of elements as used in this investigation) at an injection velocity ratio of $6\frac{1}{2}$ was constant at about $96\frac{1}{2}$ percent over a temperature range from 150° to 60° R. Thus, the apparent loss in performance with hydrogen temperature is, in fact, an injection velocity effect and can be prevented with proper injector design.

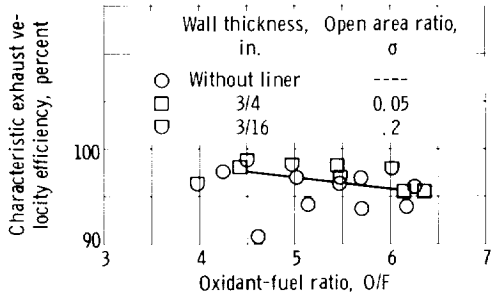

Figure 34. - Performance of 20K, H-O engine during stable combustion at hydrogen injection temperature of 120° R with 487-element coaxial injector.

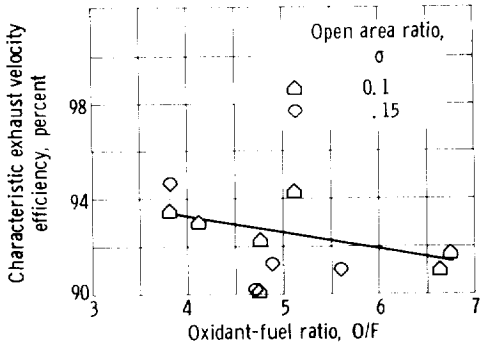

Figure 35. - Performance of 20K, H-O engine during stable combustion at hydrogen temperature of 60° R with 487-element coaxial injector with 3/16-inch-thick wall liner.

SUMMARY OF RESULTS

An investigation of suppression of high frequency combustion instability using Helmholtz type acoustic damping was conducted at the Lewis Research Center using an 20 000-pound thrust size hydrogen-oxygen engine. The tests were conducted at a chamber pressure of 300 pounds per square inch absolute (nominal) and over a range of oxidant-fuel ratios from 4 to 6. This investigation yielded the following results:

1. High frequency combustion instability in hydrogen-oxygen engines of the size investigated can be suppressed using a properly designed array of Helmholtz resonators.

2. Liner cavity gas temperature, which varied with liner variables such as aperture size, open area ratio, and axial position, has a strong effect on liner absorption characteristics. A variation in cavity gas temperature with injector element size and spacing, contraction ratio, and the propellant combination might also be expected. Thus, unless a means of predicting or controlling cavity temperature is found, no rational design procedure is possible.

3. Analytical predictions based on acoustic theory were in limited agreement with experimental results providing the effect of flow past the apertures was included in the calculation of absorption coefficient. A side velocity of 280 feet per second provided the best agreement between analytical and experimental results for a 3/16-inch-thick liner. Additional data evaluating the effect of flow past the apertures are required before liner absorption characteristics can be predicted.

4. Calculated absorption coefficients of 0.25 or higher evaluated at a cavity gas temperature typical of stable combustion and a sound pressure level of ±13 pounds per square inch were required for the injector used in the tests of eliminate screech to a hydrogen injection temperature of 60° R (minimum available).

5. Full combustor length liners were not required to suppress acoustic mode instability for the particular combustor used in the investigation. A 17 percent partial length liner positioned at the injector end of the thrust chamber provided stable combustion to a hydrogen injection temperature of 58° R.

Lewis Research Center,
National Aeronautics and Space Administration,
Cleveland, Ohio, September 26, 1966,
731-65-06-02-22.

APPENDIX - THEORY AND DESIGN OF SCREECH SUPPRESSION LINERS

In essence, screech liners are made up of an array of acoustic absorbers of the Helmholtz type. A Helmholtz resonator is an acoustic absorber consisting of a volume of gas in communication with a sound source via a small channel. If the volume is large compared to its connecting channel, the change in pressure at the entrance to the channel (resulting from incident wave(s)) will set the mass of gas in the channel in vigorous motion while the gas in the volume of the resonator is periodically compressed and rarified. The incident wave(s) energy is lost in the resonator from friction at the side walls and from turbulence near the resonator aperture. The manner in which Helmholtz resonators absorb energy can be described by an analogous mechanical system (unpublished data from G. E. Canuel) and/or by an electrical system (ref. 13). The problem of designing liners for suppression of high amplitude pressure oscillations such as are likely to occur in high output rocket combustion chambers, can be considered as one of adapting the single Helmholtz resonator theory to their design. In reference 9, some of the properties of a resonator in a free field or in a wall are presented for normal incidence of plane waves. It was also shown how the assumption of uniform wall impedance (i.e., each resonator spaced on a square array such that the distance between the centers is less than $\lambda/(2\pi)^{1/2}$) represents the limiting condition for liner design. If the distance between centers is greater than $\lambda/(2\pi)^{1/2}$, each resonator should be treated independently. The discussion thus far has been for plane waves of normal incidence in air with neither flow past the orifices nor a steady component flow through the orifices. In reference 14, it was shown that single Helmholtz resonators are effective in reducing some acoustic oscillations produced from the combustion of hydrogen and air and gasoline and air, thus extending the applicability of the theory to conditions more closely allied to those in a screeching rocket combustor (i.e., some net flow past the orifice in a medium other than air). For high amplitude pressure waves, Blackman (ref. 8) suggests a resonator array with uniform wall impedance for screech absorption liners. An array is also suggested in unpublished data from G. E. Canuel. In both unpublished data from G. E. Canuel and reference 8, the theory consists of low and high amplitude portions. For the low amplitude portion, absorption is largely a function of pressure wave amplitude when the amplitude level is less than 100 decibels. At higher levels, a resonator has a nonlinear resistance which becomes controlling. In reference 8, the nonlinear resistance has been made dependent on sound pressure level, while in unpublished data from G. E. Canuel, it is largely a function of the ratio of the particle displacement in the aperture to liner thickness. The two approaches are not entirely different since particle displacement is a linear function of the pressure amplitude. The energy absorbed by a resonator may be expressed in terms of a coefficient of absorption α, defined as the fractional part of the energy of an incident sound wave absorbed by the liner, and is dependent upon

the aperture or orifice specific acoustic resistance and reactance ratios. In the notation of reference 8, α is defined as

$$\alpha = \frac{4\theta}{(\theta + 1)^2 + x^2} \tag{A1}$$

the specific acoustic resistance ratio θ is defined as

$$\theta = \frac{r_d}{r_r} = \frac{2(2\mu\rho\omega)^{1/2}}{\sigma\rho c}\left(\epsilon + \frac{t}{d}\right) \tag{A2}$$

where

$$\epsilon = 1 + \frac{\Delta_{n\ell}}{d} \tag{A3}$$

and the specific acoustic reactance ratio x is defined as

$$x = Q\theta\left(\frac{f}{f_o} - \frac{f_o}{f}\right) \tag{A4}$$

where Q is the quality factor (measure of the liner absorption frequency bandwidth), that is,

$$Q = \frac{2\pi f_o \ell_{eff}}{\sigma c \theta} \tag{A5}$$

The liner resonant frequency f_o is given as

$$f_o = \frac{c}{2\pi}\sqrt{\frac{\sigma}{L\ell_{eff}}} \tag{A6}$$

with the effective length of the mass vibrating in the neck of the resonator defined as (unpublished data from G. E. Canuel)

$$\ell_{eff} = t + 0.85d(1 - 0.7\sqrt{\sigma}) \tag{A7}$$

In reference 8, l_{eff} is given as

$$l_{eff} = t + 0.85d(1 - 0.7\sqrt{\sigma}) - \delta \tag{A8}$$

where δ is an end correction factor. In this instance, δ is a function of the open area ratio σ. It decreases with increasing values of σ until an open area ratio of approximately 6 percent is reached; thereafter, δ remains a constant. The design procedure reported herein uses equations (A1), (A2), and (A4) to (A7) with the nonlinear resistance term ϵ evaluated as a function of the ratio of the particle displacement to the plate thickness (ref. 9). The particle displacement as used herein and as given in unpublished data from G. E. Canuel is

$$X_o = \frac{2P_i}{\frac{\rho c^2 \sigma}{Lg}} \left\{ \frac{1}{\sqrt{\left[1 - \left(\frac{\omega}{\omega_o}\right)^2\right]^2 + \left(\frac{R\omega}{\rho l_{eff} \omega_o^2}\right)^2}} \right\} \tag{A9}$$

with R defined as

$$R = (1 + \theta)\sigma\rho c \tag{A10}$$

Several modifications have been made to the procedure for flow of gas particles past or through the orifices. For flow through, equation (A2) becomes (ref. 15)

$$\theta = \frac{2(2\mu\rho\omega)^{1/2}}{\sigma\rho c}\left(\epsilon + \frac{t}{d}\right)(0.305V - 0.72) \tag{A11a}$$

and, for flow past the orifice, equation (A2) becomes (ref. 16)

$$\theta = \frac{2(2\mu\rho\omega)^{1/2}}{\sigma\rho c}\left(\epsilon + \frac{t}{d}\right)(1 - A_f U)^{-4} \tag{A11b}$$

The parameter A_f was shown in reference 6 to be frequency dependent. Presently, there are no correlations for the combined effects of flow past and flow through the orifices. Partitions behind the liner can be used to prevent net flow through of particles;

consequently, the designer will use either equation (A2) or (A11b). If the velocity past the orifices is small, equation (A11b) gives approximately the same results as equation (A2).

The equations described are best solved on a high-speed computer and were, therefore, programmed for solution on the Lewis Research Center IBM 7090 digital computer. The original program was received from Pratt and Whitney Aircraft Division of United Aircraft Corporation.

REFERENCES

1. Phillips, Bert, and Morgan, C. Joe: Mechanical Absorption of Acoustic Oscillations in Simulated Rocket Combustion Chambers. NASA TN D-3792, 1966.

2. Usow, Karl H.; Meyer, Carl L.; and Schulze, Frederick W.: Experimental Investigation of Screeching Combustion in Full-scale Afterburner. NACA RM E53I01, 1953.

3. Harp, James L., Jr.; Velie, Wallace W.; and Bryant, Lively: Investigation of Combustion Screech and Method of Its Control. NACA RM E53L24b, 1954.

4. Backshear, Perry R.; Rayle, Warren D.; and Tower, Leonard K.: Study of Screeching Combustion in a 6-inch Simulated Afterburner. NACA TN 3567, 1955.

5. Lawhead, R. B.; and Levine, R. S.: Rocket Engine Vibration Studies. Project MX 919. Rep. No. RE-134, North American Aviation, Inc., July 15, 1954.

6. Utnik, D. H.; Ford, H. J.; and Blackman, A. W.: Evaluation of Absorption Liners for Suppression of Combustion Instability in Rocket Engines. J. Spacecraft, vol. 3, no. 7, July 1966, pp. 1039-1045.

7. Wanhainen, John P.; Parish, Harold C.; and Conrad, E. William: Effect of Propellant Injection Velocity on Screech in 20,000-Pound Hydrogen-Oxygen Rocket Engine. NASA TN D-3373, 1966.

8. Blackman, A. W.: Effect of Nonlinear Losses on the Design of Absorbers for Combustion Instabilities. ARS J. vol. 30, no. 11, Nov. 1960, pp. 1022-1028.

9. Ingaard, Uno: On the Theory and Design of Acoustic Resonators. Acoust. Soc. Am. J., vol. 25, no. 6, Nov. 1953, pp. 1037-1061.

10. Crocco, Luigi; and Cheng, Sin-I: Theory of Combustion Instability in Liquid Propellant Rocket Motors. Butterworth Scientific Publ., 1956.

11. Hefner, R. J.: Review of Combustion Stability Development with Storable Propellants. Paper No. 65-614, AIAA, June 1965.

12. Zwikker, C.; and Kosten, C. W.: Sound Absorbing Materials. Elsevier Publ. Co., Inc., 1949.

13. Morse, Philip M.: Vibration and Sound. 2nd ed., McGraw-Hill Book Co., 1948.

14. Putnam, A. A.; and Dennis, W. R.: Suppression of Burner Oscillations by Acoustical Dampers. ASME Trans., vol. 77, no. 6, Aug. 1955, pp. 875-883.

15. McAuliffe, Clinton E.: The Influence of High Speed Air Flow on the Behavior of Acoustical Elements. M.S. Thesis, M.I.T., 1950.

16. Mechel, F.; and Schilz, W.: Research on Sound Propagration in Sound-Absorbent Ducts with Superimposed Air Streams. Vol. II. Rep. No. AMRL-TDR-62-140 (II), U.S. Air Force, W-PAFB, Biomediceil Lab., Dec. 1962. (Available from DDC as AD296985.)